Title

Virus Control in Vaccinated Rhesus Macaques Is Associated with Neutralizing and Capturing Antibodies against the SHIV Challenge Virus but Not with V1V2 Vaccine–Induced Anti-V2 Antibodies Alone

Journal

The Journal of Immunology, 206(6)

ISSN

0022-1767

Authors

Hessell, Ann J
Li, Liuzhe
Malherbe, Delphine C
et al.

Publication Date

2021-03-15

DOI

10.4049/jimmunol.2001010

Peer reviewed

HHS Public Access

Author manuscript

J Immunol. Author manuscript; available in PMC 2022 March 15.

Published in final edited form as:

J Immunol. 2021 March 15; 206(6): 1266–1283. doi:10.4049/jimmunol.2001010.

Virus control in vaccinated rhesus macaques is associated with neutralizing and capturing antibodies against the SHIV challenge virus but not with V1V2 vaccine-induced anti-V2 antibodies alone

Ann J. Hessell[*], **Liuzhe Li**[†], **Delphine C. Malherbe**[*], **Philip Barnette**[*], **Shilpi Pandey**[*], **William Sutton**[*], **David Spencer**[*], **Xiao-Hong Wang**[‡], **Johannes S. Gach**[§], **Ruth Hunegnaw**[¶], **Michael Tuen**[†], **Xunqing Jiang**[‖], **Christina C. Luo**[‖], **Celia C. LaBranche**[#], **Yongzhao Shao**[**], **David C. Montefiori**[#], **Donald N. Forthal**[§], **Ralf Duerr**[†], **Marjorie Robert-Guroff**[¶], **Nancy L. Haigwood**[*], **Miroslaw K. Gorny**[†]

[*] Oregon National Primate Research Center, Oregon Health & Science University, Beaverton, Oregon, USA

[†] Department of Pathology, New York University School of Medicine, New York, New York, USA

[‡] Veterans Affairs New York Harbor Healthcare System, New York, New York, USA

[§] Department of Medicine, Division of Infectious Diseases, University of California, Irvine School of Medicine, Irvine, California, USA

[¶] Vaccine Branch, National Cancer Institute, National Institutes of Health, Bethesda, Maryland, USA

[‖] Department of Biochemistry & Molecular Pharmacology, New York University School of Medicine, New York, New York, USA

[#] Division of Surgical Sciences, Duke University, Durham, North Carolina, USA, USA.

[**] Department of Population Health, New York University School of Medicine, New York, New York, USA

Abstract

The role of vaccine-induced anti-V2 antibodies (Abs) was tested in three protection experiments in rhesus macaques. In an experiment using immunogens similar to those in the RV144 vaccine trial, (Anti-Env) nine rhesus macaques were co-immunized with $gp160_{92TH023}$ DNA and SIV gag, $gp120_{A244}$ and $gp120_{MN}$ proteins. In two V2-focused experiments (Anti-V2 and Anti-V2 Mucosal), nine macaques in each group were immunized with $V1V2_{92TH023}$ DNA, $V1V2_{A244}$ and $V1V2_{CasaeA2}$ proteins, and cyclic $V2_{CaseA2}$ peptide. DNA and protein immunogens, formulated in Adjuplex, were given at 0, 4, 12 and 20 weeks, followed by intrarectal $SHIV_{BaL.P4}$ challenges.

Address correspondence to Dr. Miroslaw K. Gorny, Department of Pathology, New York University School of Medicine, New York, NY 10016. mirek.gorny@nyulangone.org.

Disclosures

None of the authors declares conflicts of interest.

The online version of this article contains supplemental data.

Peak plasma viral loads (PVL) of 10^6–10^7 copies/mL developed in all nine sham controls. Overall, PVL was undetectable in one-third of immunized macaques, and two animals tightly controlled the virus with the Anti-V2 Mucosal vaccine strategy. In the Anti-Env study, antibodies that captured or neutralized $SHIV_{BaL.P4}$ inversely correlated with PVL. Conversely, no correlation with PVL was found in the Anti-V2 experiments with non-neutralizing plasma Abs that only captured virus weakly. Titers of Abs against eight V1V2 scaffolds and cyclic V2 peptides were comparable between controllers and non-controllers as were ADCC and ADCVI activities against SHIV-infected target cells and phagocytosis of gp120-coated beads. The Anti-Env experiment supports the role of vaccine-elicited neutralizing and non-neutralizing Abs in control of PVL. However, the two V2-focused experiments did not support a role for non-neutralizing V2 Abs alone in controlling PVL, as neither ADCC, ADCVI nor phagocytosis correlated inversely with heterologous $SHIV_{BaL.P4}$ infection.

Keywords

HIV vaccine; V2 antibody; V1 antibody; HIV neutralizing antibody; virus capture antibody; ADCC; ADCVI; phagocytosis; mucosal antibodies; SHIV challenge; immune correlates; V1V2 fusion proteins; cyclic V2 peptides

Introduction

In the RV144 HIV vaccine trial, which achieved a modest efficacy of 31.2%, the only immune response associated with a reduction in HIV-1 infection was a high level of plasma anti-V2 antibodies (V2 Abs) (1). This result suggested that V2 Abs contribute to protection against HIV-1 infection, although the protection mechanism remains unknown. Efforts to replicate the efficacy of the RV144 trial findings using similar vaccines in the setting of clade C immunogens in the HVTN 702 clinical trial failed to show differences in HIV acquisition between the vaccine and placebo arms (2). Thus, understanding the role of specific V2-directed envelope (Env) Abs in protection remains a crucial question.

V2 Abs mainly target Tier 1 viruses and mediate several antiviral functions that may contribute to protection, whereas in the RV144 clinical trial, 89% of infections occurred with Tier 2 CRF01_AE strains (3). Neutralizing Abs (NAbs) are critical for protection against many viruses, including HIV-1 (4, 5). Tier-1 neutralizing V2 monoclonal Abs (mAbs) have comparable neutralizing capacity as V3 mAbs and some CD4bs mAbs. These three types of Abs are commonly induced by natural HIV infection and experimental vaccines, but are not broadly neutralizing and rarely neutralize Tier 2 HIV-1 (6–10).

Nonetheless, V2 Abs can mediate effector functions through the Fc fragment *in vitro*, such as antibody-dependent cellular phagocytosis (ADCP) and antibody-dependent cellular cytotoxicity (ADCC), and these functions potentially modulate infection *in vivo* (11). A study comparing the capacity of mAbs directed to different regions of HIV-1 Env for mediating phagocytosis revealed that V2 mAbs exhibited comparable activity to mAbs against V3 and the CD4bs (12). Immunization of rabbits and rhesus macaques using V1V2 scaffold proteins elicited V2 Abs that infrequently mediated phagocytosis depending on the animal group and immunogen tested (13, 14). ADCC activity mediated by V2 mAbs was

limited in most studies (9, 15, 16). Vaccine-induced V2 Abs in rhesus macaques were able to mediate ADCC sporadically (14). The contribution of phagocytosis and ADCC to protection in several rhesus macaque challenge experiments is still under investigation and rarely correlated with virus acquisition (17–19).

A unique function of V2 mAbs is the ability to bind to the α4β7 integrin-binding site in the V2 region and inhibit the interaction between α4β7 integrin and gp120 or V2 peptide *in vitro* (20, 21). Other findings suggested that V2 Abs *in vivo* may block viral adhesion and subsequent infection of Th17 cells expressing CD4, CCR5, and α4β7 integrin (22, 23). This concept was tested in three experiments in rhesus macaques and one clinical trial in humans that showed an anti-α4β7 mAb could not sustain the suppression of viral load upon discontinuation of all treatments (24–27). Furthermore, in one of these studies, two rhesus V2 mAbs that blocked binding of SIV Env to α4β7 did not control SIV infection in rhesus macaques (26).

We tested the protective capacity of a single human V2 mAb (830A) by passive transfer to rhesus macaques with subsequent mucosal $SHIV_{BaL.P4}$ challenges. In that study, plasma viral load (PVL) and viral DNA in PBMCs and lymphoid tissues were reduced, but the number of infected animals was not reduced compared to controls (16). These results are comparable to three other passive immunization experiments in rhesus macaques that showed non-neutralizing Abs specific to CD4bs, C1 region of gp120, and against gp41 may reduce PVL, but unlike experiments with broadly neutralizing monoclonal Abs (bNAbs), cannot protect against virus infection (28–30).

Here, we performed three separate protection experiments in rhesus macaques to address whether vaccine-induced V2 Abs in rhesus macaques can control a heterologous Tier 1 $SHIV_{BaL.P4}$ challenge. The first experiment, termed Anti-Env, was intended to determine whether co-immunization with a DNA/protein regimen could mimic the correlation between V2 Abs and the reduced risk of infection reported in the RV144 vaccine trial. The second and third experiments, termed Anti-V2 and Anti-V2 Mucosal, tested the ability of V2-focused Abs induced systemically and mucosally, respectively, to protect against intrarectal challenge. The studies showed that V2 Abs did not independently control $SHIV_{BaL.P4}$ infection. Neither V2 Ab binding titers nor functional activities of phagocytosis, ADCC or antibody-dependent cell-mediated virus inhibition (ADCVI) correlated with plasma viral load or $SHIV_{BaL.P4}$ acquisition.

Material and Methods

Ethics Statement.

Experiments in this study were performed in accordance with the Guide for the Care and Use of Laboratory Animals of the National Institutes of Health, the Office of Animal Welfare, and the U.S. Department of Agriculture. All experiments on animals have been reviewed and approved by the Institutional Animal Care and Use Committee at the Oregon Health and Science University (OHSU) and the New York University School of Medicine, New York, NY. The American Association accredits the Oregon National Primate Research Center (ONPRC) for Accreditation of Laboratory Animal Care.

Animals.

A total of thirty-six rhesus macaques (*Maccaca mulatta*), comprised of twenty-two females and 14 males, between 3 and 9.7 years of age were housed at the ONPRC in Beaverton, OR and used in the study. All animals were free of cercopithicine herpesvirus 1, D-type simian retrovirus, simian T-lymphotropic virus type 1, and SIV infection at the start of the study. Macaques were genotyped for MHC class I alleles *Mamu*-A*01, -A*02, B*01, -B*08, and -B*17 (Table I).

Generation of the 92TH023/VC10014_F8 gp160 vaccine construct and V1V2 DNA.

The motif-optimized (MO) 92TH023/VC10014_F8 gp160 DNA chimera was generated by in-frame cloning of 92TH023 gp120 with VC10014_F8 gp41. The gp120 DNA sequence of HIV envelope 92TH023 (GenBank accession number EF553537; https://www.ncbi.nlm.nih.gov/nuccore/EF553537) was first MO with the Robins–Krasnitz algorithm as previously described (31, 32) and then synthesized (Blue Heron, Bothell, WA). Using NheI and BmgbI restriction sites, replacement cloning was performed to swap the MO VC10014_F8 gp120 with the MO 92TH023 gp120 fragment so that MO 92TH023 gp120 was cloned in frame with MO VC10014_F8 gp41 in the pEMC* expression vector; the isolation and cloning of HIV envelope VC10014_F8 (GenBank accession number KJ698264; https://www.ncbi.nlm.nih.gov/nuccore/KJ698264) were described in (33). The DNA sequence and in-frame cloning of MO 92TH023/VC10014_F8 gp160 were confirmed by Sanger sequencing. The MO 92TH023/VC10014_F8 gp160 chimera was functional since it produced an infectious pseudovirus by complementing the pSG3ΔEnv backbone DNA plasmid (34). $V1V2_{92TH023}$ DNA with additional nucleotides coding for five amino acids (AA) at each end was produced in the same laboratory and used for the two protection experiments, Anti-V2 and Anti-V2 Mucosal.

Immunogens.

Two recombinant gp120 proteins, $gp120_{A244}$ (CRF01_AE) and $gp120_{MN}$ (clade B) were used for co-immunization with DNA in the first protection experiment (Anti-Env). The recombinant $gp120_{A244}$ was produced using a plasmid provided by Dr. X-H. Liao, Duke University, and modified by an N-terminal 11-amino-acid deletion (Δ11) and addition of an HSV gD protein-and derived tag (gD). For the Anti-V2 and Anti-V2 Mucosal experiments, V1V2 scaffolds, $V1V2_{A244}$-2F5K and $V1V2_{Case\ A2}$-2F5K, were produced as described (35) and cyclic $V2_{Case\ A2}$ peptide was produced by Biopeptide Co, Inc, San Diego, CA.

Recombinant proteins, V1V2 proteins and V2 peptides.

Three recombinant proteins, $gp120_{MN}$, $gp120_{BaL}$ and $V1V2_{Case\ A2}$-gp70 (clade B), were purchased from Immune Technology Corp., New York, NY. $V1V2_{ZM109}$-1FD6, $V1V2_{A244}$-2F5K and $V1V2_{1086}$-tags (clade C) were produced as previously described (35). Biotinylated cyclic peptides, $V2_{BaL}$, $V2_{CaseA2}$ (clade B), $V2_{230}$ (CRF02_AG), $V2_{A244}$ (clade AE) and $V1_{92TH023}$ (clade AE) were purchased from Biopeptide Co., Inc., San Diego, CA.

Animal immunization.

Macaques were co-immunized at weeks 0, 4, 12, and 20 with 36 μg of HIV DNA and 36μg of SIV *gag* delivered intradermally (ID) and soluble proteins delivered intramuscularly (IM). The recombinant proteins were delivered along the shaved abdomen and one or more proteins delivered in the quadriceps. The Anti-Env group received $gp160_{92TH023}$ DNA plus $gp120_{A244}$ and $gp120_{MN}$ recombinant proteins. In the Anti-V2 and Anti-V2 Mucosal groups, animals were co-immunized with $V1V2_{92TH023}$ DNA (ID) and $V1V2_{A244}$-2F5K, $V1V2_{Case\ A2}$-2F5K proteins with cyclic $V2_{Case\ A2}$ peptide, 50 μg each formulated in adjuvant (Adjuplex). The proteins were delivered IM in the Anti-V2 group and by intranasal atomized spray in the Anti-V2 Mucosal group (Fig. 1). The DNA immunogens were delivered via the Particle Mediated Epidermal Delivery (PMED) Gene Gun, a machine that shoots gold “bullets” consisting of 1-micron beads with dried DNA on the surface (PowderJect XR1, developed by PowderMed, Ltd., Oxford, UK). The bullets were shot under the abdomen’s skin to target inguinal lymph nodes nearby or gut-associated lymphoid tissue (GALT). During the same procedure, we injected protein immunogens (approximately 0.1 ml volume) into the quadriceps or sprayed with an atomizer into the nasal cavity.

Protection study.

Protection experiments were performed on three groups, nine animals each, of immunized rhesus macaques at the Oregon National Primate Research Center, Beaverton, OR. The three control groups of three macaques each were immunized with vector DNA only (sham) to serve as a control group for virus infection. The challenge virus was propagated in PHA-stimulated macaque PBMC and titrated *in vivo*. A stock of $SHIV_{BaL.P4}$ was obtained through collaboration with Dr. Sampa Santra, Beth Israel Deaconess Medical Center, Boston, MA. The $SHIV_{BaL.P4}$ isolate was propagated in human PBMCs to generate a large volume stock for rhesus challenge experiments. The mean genetic diversity of Env determined by single genome sequencing in this stock is 0.3%, with a maximum diversity of 0.7% (29).

Animals were challenged with $SHIV_{BaL.P4}$ two weeks after the fourth immunization at week 22 of the experiment. The virus stock was diluted and dosed at $TCID_{50}$ of ~6×10^5 based on the *in vivo* titration data provided by Dr. Santra. Two repeated intrarectal (IR) exposures given one week apart resulted in a productive infection of all three sham vaccinated animals in the Anti-Env group. Five repeated IR exposures were required to infect controls for the Anti-V2 and Anti-V2 Mucosal experiments.

Detection of virus in plasma, PBMCs and lymph nodes.

Detection and quantification of SIV *gag* viral RNA (vRNA) to monitor the onset of infection were performed as described (16). Briefly, viral loads in plasma were measured by quantitative reverse transcription-PCR (RT-PCR) (36), whereas viral loads in PBMC DNA were quantitated by PCR using Fast Advanced Mastermix on an Applied Biosystems QuantStudio 6 Flex instrument (Life Technologies, Carlsbad, CA). The detection of vRNA and DNA in lymph nodes was determined by ultrasensitive nested quantitative PCR and RT-PCR methods (37).

Binding assays.

Macaque plasma samples were screened against antigens using a standard ELISA as described (38). Briefly, V1V2 scaffold proteins were coated directly onto plastic plates at a concentration of 1 μg/mL, while biotinylated cyclic V2 and V1 peptides were immobilized on streptavidin-coated plates (StreptaWell plates, Roche). The plates were washed and blocked with assay diluent (PBS containing 2.5% bovine serum albumin and 7.5% fetal bovine serum) and then incubated with plasma samples diluted eight times ranging from 1:10 to 1:30,000. After washing, the bound Abs were detected by incubation with alkaline phosphatase-conjugated goat anti-human IgG (γ specific) (Southern Biotech) followed by washing and adding substrate to develop color. Mucosal secretions, buccal and vaginal, were tested by ELISA for Abs that bind to $gp120_{BaL}$, $gp120_{MN}$ and $V1V2_{1086}$-tags; the second antibody was peroxidase-conjugated goat anti-human IgG (γ specific) (Jackson Immuno Research).

Virus capture assay.

Virus capture assays were carried out according to Gach et al. (39). Briefly, 96 well half-area plates (Corning) were coated with 250 ng per well of a goat anti-monkey IgG gamma chain-specific antibody (Rockland) and incubated overnight at 4°C. Wells were washed and subsequently blocked with 5% nonfat dry milk in PBS. After blocking, plasma samples (50 μL of 1:100 dilution per well) were incubated for one hour at 37°C before adding $SHIV_{BaL.P4}$ (1 ng p27/well) for another four hours at 37°C. Plates were finally washed five times with PBS and TZM-bl reporter cells were added (1×10^4 cells per well) supplemented with 15 μg/mL of DEAE-dextran. After three days of incubation at 37°C, cells were washed, lysed, and analyzed for luminescence (BioTek) after adding luciferase assay reagent (Promega). Capture assays were performed twice in duplicate wells.

Neutralization assay.

The neutralizing activities of plasma Abs against $SHIV_{BaL.P4}$ and nine other pseudotyped viruses and the SVA-MLV negative control pseudovirus were tested using the standard TZM-bl cell assay (38, 40, 41). Briefly, plasma samples were heat-inactivated and titrated at 3-fold dilutions starting at 1:50 and then pre-incubated with the virus at an input of 200 $TCID_{50}$ for 1 h. The virus/plasma Abs mixtures were then incubated for 48 h with TZM-bl cells. Virus infectivity was determined by measuring luciferase activity in cell lysates. The 50% inhibitory dilution (ID_{50}) was determined that resulted in a 50% reduction in relative light units (RLU) compared to wells with the virus only, after the subtraction of cell control RLUs (8, 41). All plasma samples were tested in duplicate. A pool of the pre-immune plasma was used as a negative control. Neutralization dose-response curves were fitted by non-linear regression.

Antibody-dependent cellular cytotoxicity (ADCC).

The assay was performed as described by Hessell et al. (16), and adapted from Alpert et al. (42). Briefly, NKR24 target cells were infected with $SHIV_{SF162p3}$ and incubated for 3 to 4 days before the start of the assay to achieve an infection titer at least five times over the background. Infected target cells were combined with KHYG-1 rhCD16 cells, derived from

the CD16-negative human NK cell line KHYG-1, at an effector-to-target cell (E:T) ratio of 5:1, and added to the assay plate along with serially diluted macaques plasma samples, and positive and negative mAb controls that define 100% and 0% RLU were included. The assay mixture was incubated for 8 h, after which the Bright-Glo luciferase substrate reagent (Promega) was used to read activity. The data were quantified by 50% ADCC titers and AUC values for ADCC.

Antibody-dependent cellular phagocytosis (ADCP).

Phagocytosis activity was measured as previously described (43) with minor modifications. In short, HIV-1 $gp120_{BaL}$ was biotinylated with a Biotin-XX microscale protein labeling kit (Thermo Fisher Scientific, Waltham, MA) and incubated with a 100-fold dilution of 1 μg yellow-green streptavidin-fluorescent beads (Thermo Fisher Scientific) overnight at 4°C in the dark. A 1:25, 1:50, 1:100 and 1:200 dilution of plasma samples from each macaque was added to 400,000 THP-1 cells, plated in a U-bottom 96-well plate. The bead-gp120 mixture was further diluted 5-fold in R10 media, and 50 μL was added to the cells. The mix was incubated for 3 h at 37°C and fixed with 70 μL of 2% paraformaldehyde. Fluorescent bead uptake by THP-1 cells was assessed using a BD Biosciences LSRII flow cytometer (BD Biosciences, San Jose, CA). The phagocytic score of each sample was calculated by multiplying the percentage of bead-positive cells (frequency) by the degree of phagocytosis measured as mean fluorescence intensity (MFI) and dividing by 10^6. Values were normalized to background values (cells and BSA coated beads) by dividing the phagocytic score of the test sample by the phagocytic score of the background sample.

Antibody-dependent cell-mediated virus inhibition (ADCVI) assay.

ADCVI assays were performed as previously described (44). In brief, heat-inactivated plasma samples were initially diluted 1:25 with medium (final dilution of 1:100) before adding $SHIV_{BaL.P4}$-infected CEM.NKr-CCR5 target cells and freshly isolated human peripheral mononuclear effector cells at an effector/target ratio of 10:1. After three days of incubation, Abs were removed by washing wells three times with PBS. Four days later, cell-free supernatants were collected and analyzed by a SIV p27 ELISA. Each plasma sample was assayed in triplicate, and the ADCVI activity (percent ADCVI) of week 14 and week 22 samples was calculated relative to the respective week 0 samples. ADCVI assays were repeated at least twice.

Envelope sequencing of plasma breakthrough $SHIV_{BaL.P4}$.

Plasma viruses from nine non-controllers from two protection studies, one sham animal, and the challenge virus ($SHIV_{BaL.P4}$) were sequenced in the envelope protein region to analyze sites of immune pressure in the breakthrough viruses in comparison to controls. For each analyzed animal, sequence analysis was performed for the virus bulk sequence and five clones (pCR4 TOPO). Amplification, cloning into pCR4 TOPO and sequencing was based on an established protocol (45) with minor changes. Briefly, vRNA was extracted from the plasma sample using the QIAamp mini kit (Qiagen Inc., Valencia, CA). Reverse transcription was performed using primer SHIV 10231 rev (5'-ACAGAGCGAAATGCAGTGATATT-3') and GoScript (Promega) Reverse Transcriptase according to the manufacturer's instructions. Nested PCRs were performed over the full *env*

region, according to HIV-1 HXB2 region 6225–8802 (~2600 bp) using PrimeSTAR GXL DNA polymerase (Clontech) with primers EnvB (5'-AGAAAGAGCAGAAGACAGTGGCA-3') and SHIV 10231 rev in 1st Round PCR, and platinum *Taq* polymerase (Invitrogen, Carlsbad, CA) with newly designed primers SHIV Env1 (5'-ATGAGAGTGACGGAGATCAGGA-3') and SHIV 8496 rev (5'-ACCCATATTGTAGGTAGGCTCG-3') in 2nd Round PCR. Bulk sequencing was performed with SHIV Env1, SHIV 8496 rev, For15, Rev15, and/or Rev 17 (46). Additionally, PCR products were cloned into the pCR4 TOPO cloning vector (Life Technologies, Carlsbad, CA) and transformed into One Shot TOP10 competent *E. coli*. Plasmids were sequenced for the insert portion using universal primers M13F, M13R, and For15. Sequence analysis and alignment were performed using SeqMan Pro (DNASTAR), MEGA5.2 with Muscle (47) and MegAlign (DNASTAR).

Statistical analysis.

The 50% titers of plasma Abs and area under the curves (AUC) for two groups of animals, controllers and non-controllers of $SHIV_{BaL.P4}$ infection, were compared by the nonparametric Mann-Whitney tests. Group comparison significance was determined by One-way ANOVA. The nonparametric Spearman's test with P values (two-tailed) and linear regression were used to assess the correlation between the results of neutralization, capture Abs, AUC and PVL. A log-rank test was used to analyze the Kaplan-Meier curves and evaluate differences between controllers and non-controllers. Fisher's exact test was used to determine the significance of controllers in vaccinated animals. The statistical analyses were performed using GraphPad Prism.

Results

Vaccine/challenge experiments in rhesus macaques

Three groups of nine animals each were co-immunized at weeks 0, 4, 12, and 20: intradermally (ID) with HIV and SIV *gag* DNA, and either intramuscularly (IM) or mucosally with a nasal spray (IN) of soluble proteins and peptide. All proteins were formulated with Adjuplex adjuvant. The first experiment (Anti-Env) was designed to loosely mimic the RV144 vaccine with macaques co-immunized with chimeric $gp160_{92TH023}$ DNA, plus $gp120_{A244}$ and $gp120_{MN}$ proteins. The Anti-Env group served as a positive control for two vaccine groups designed to induce only V1V2 Abs (Anti-V2 and Anti-V2 Mucosal). The Anti-V2 and Anti-V2 Mucosal groups were co-immunized with $V1V2_{92TH023}$ DNA (ID) plus V1V2-scaffold proteins $V1V2_{A244}$-2F5K, $V1V2_{CaseA2}$-2F5K, and the cyclic $V2_{CaseA2}$ peptide. These groups differed only in the route of protein immunogen delivery, IM (Anti-V2) or IN (Anti-V2 Mucosal). The V2 peptide was included with the last two immunizations to enhance the induction of Abs against V2 linear antigens (Fig. 1). Controls for each group consisted of three non-human primates (NHP), each receiving an empty plasmid sham vaccine at week 20. Controls were subsequently challenged simultaneously with vaccinated animals. $SHIV_{BaL.P4}$ at a median tissue culture infectious dose ($TCID_{50}$) of ~6×10^5 was administered intrarectally (IR) to all animals starting at week 22. We designed these studies under the criterion that challenges would cease when all controls were infected, and we followed this strategy for all three groups. Based on previous experiments, the SHIV

BaL stock at the dilution used here was expected to infect sham-vaccinated controls after 3–4 IR challenges. Surprisingly, only a single challenge was required to infect controls and one vaccinated macaque in the Anti-Env experiment. Therefore, challenges were stopped after two challenges. We were unable to run all three experiments concurrently, and the Anti-V2 and Anti-V2 Mucosal V2 groups received five SHIV challenges before all controls were infected (Fig. 1).

PVL was determined weekly by measuring SIV *gag* vRNA. Peak PVL reached 10^6 to 10^7 copies/mL in control animals 2–3 weeks post the first challenge in the Anti-Env group. In the Anti-V2 and Anti-V2 Mucosal groups, peak PVL was recorded 3–5 weeks post the first challenge. The reason for the variation in the number of challenges required to infect the controls between the Anti-Env group and the Anti-V2 groups was undetermined. The virus stock $SHIV_{BaL.P4}$ $TCID_{50}$ was re-checked on three separate occasions during repeated challenges and found to be comparable.

In the Anti-Env group, five of nine (55%) vaccinated animals controlled viremia. PVL was undetectable in four of these five animals except for a single blip (a signal that appears at a single time point) of 68–360 vRNA copies/mL (30300, 33615, 33620, 33653). Three PVL blips were detected in the plasma of the fifth Anti-Env group controller (33617) ranging from 140 to 1200 vRNA copies/mL (Fig. 2A). PVL was undetectable in four of nine animals (44%) in the Anti-V2 group (31467, 33607, 34149, 34209) and two of nine animals (22%) in the Anti-V2 Mucosal groups, indicating control of viremia in these animals (Fig. 2A). Cell-associated SIV *gag* DNA was also undetectable in PBMCs from the vaccinated macaque controllers (Fig. 2B) and axillary, mixed mesenteric, iliosacral, and inguinal lymph nodes collected at necropsy (Fig. 2C).

A comparison by group of the mean of all tissue-associated virus underscores the substantial reduction in virus distribution provided by the Anti-Env vaccine. In the draining lymph nodes tested, the increased SIV vDNA per 1×10^6 cells examined in the Anti-V2 and Anti-V2 Mucosal groups was highly significant compared to the Anti-Env group ($p<0.0001$) (Fig. 2C). The tissue-associated virus was comparable in the Anti-V2 and Anti-V2 Mucosal groups ($p=0.2242$), but it was significantly higher in sham controls compared to all vaccinated macaques ($p<0.0001$).

A Kaplan-Meier analysis of productive infections occurring in non-controllers after each SHIV IR challenge revealed that only the Anti-Env vaccine resulted in a significant difference between controllers (56%, $p=0.0068$) and non-controllers. For the Anti-V2 and Anti-V2 Mucosal groups, (44%, $p=0.0497$ and 22% $p=0.3703$), respectively, of controllers remained after the number of SHIV challenges required to infect controls (Fig. 2D).

Macaque MHC class I alleles

We genotyped class I MHC *Mamu*-A and B alleles in all 36 rhesus macaques used in the study to define whether the genetic background may impact SHIV infection progression (Table I). Four MHC *Mamu*-A alleles were detected: *Mamu*-A1*001:g, associated with reduced loss of $CD4^+$T cells and longer survival (48), was detected in two controllers (31467 and 34578), and *Mamu*-A1*002:g, associated with longer survival (49), was detected in two

non-controllers (32669 and 32672). *Mamu*-B*001:g, which has not been associated with elite controllers (50), was present in six animals: three non-controllers (32669, 32672, 32037), and three sham animals (30262, 32661, 32195) (Table I). *Mamu*-B*008:g and *Mamu*-B*017:g alleles were not detected in any animals. In summary, two alleles that may suppress SHIV infection, *Mamu*-A1*001:g and *Mamu*-A1*002:g, were present in both controllers and non-controllers, whereas *Mamu*-B*001:g was present in sham controls with both high (32661) and low PVL (30262) (Table I). Based on these observations, we consider it unlikely that these three MHC alleles influenced PVL.

Sites of immune pressure in Env revealed by mutations in plasma breakthrough viruses from non-controllers

The identities of point mutations in the envelope region in plasma viruses from immunized and non-controllers can reveal the selection pressure from Abs induced by vaccine on the challenge virus. Accordingly, we obtained plasma samples at peak PVL (weeks 25–29) from nine non-controllers from the Anti-Env and Anti-V2 groups and from sham-vaccinated controls. The Anti-V2 Mucosal samples were not included. We aligned the *env* gene sequences with those from $SHIV_{BaL.P4}$ challenge virus (Table II). The majority of the point mutation sites (18 of 23) were located in the conserved regions of gp120, C1 to C4, with two mutations in V1 and V2 each and one in the V3 region (Table II). V254L in the C2 region of gp120 was the most common mutation site in or near the CD4bs; it was present in five out of nine animals and presumably induced by anti-CD4bs Abs.

Immune pressure on the V2 region was minimal, indicating the mutations were induced by *de novo* Abs to the $SHIV_{BaL.P4}$ during infection. The deletions at positions 189/190 were detected in the hypervariable part of the V2 (Anti-Env, 32672) that could be induced exclusively by homologous Abs elicited by $SHIV_{BaL.P4}$. Abs to the challenge virus also probably led to the point mutation K168E in the Anti-V2 experiment, and an additional 11 mutations outside of the V2 in the Anti-V2 study, although it is possible that Abs elicited by the V1V2 vaccine against V2 could have resulted in this mutation. Mutation sites in C1 and C2 in sham controls likely reflect the other constant region changes in the Anti-Env and Anti-V2 groups and generally supports the conclusion that the mutations found were essentially induced by Ab responses to the challenge virus (Table II).

Binding of plasma antibodies to V1V2 scaffold proteins and cyclic V2 peptides

We measured the binding of titrated plasma samples collected at week 22, the time of the first challenge (TOC), from each group, Anti-Env, Anti-V2 and Anti-V2 Mucosal, against four V1V2 scaffold proteins and four biotinylated cyclic V2 (cV2) peptides (Supplementary Fig. 1). Midpoint plasma Ab titers were binned and analyzed by three methods. First, individual animal responses against each V1V2 scaffold protein representing clades B, C, and AE ($V1V2_{CaseA2}$-gp70, $V1V2_{1086}$-tags, $V1V2_{ZM109}$-1FD6 and $V1V2_{A244}$-2F5K) were compared by the group. Ab titers in the Anti-V2 group were significantly higher compared to titers in the Anti-Env group and the Anti-V2 Mucosal group (**$p<0.01$) (Fig. 3A). Next, group responses were compared against each V1V2 scaffold protein. Ab titers in the Anti-V2 group were consistently highest among the groups against all of the V1V2 proteins tested. Ab titers to $V1V2_{CaseA2}$-gp70 and $V1V2_{1086}$-tags in all Anti-V2 macaques exceeded

1000 and were significantly higher than Ab titers in either the Anti-Env or Anti-V2 Mucosal groups (***p<0.001) (Fig. 3B). V1V2 scaffold proteins induced comparable titers in the Anti-Env and Anti-V2 Mucosal groups. The lowest titers in all groups were against the $V1V2_{ZM109}$-1FD6 scaffold protein.

We determined Ab titers from serially diluted plasma against four cV2 peptides ($cV2_{CaseA2}$, $cV2_{230}$, $cV2_{A244}$, $cV2_{BaL}$) for individual animals in each group (Fig. 3C). Similar to the pattern seen with responses against the V1V2 scaffold proteins, binding Ab titers to each cV2 peptide were significantly higher in the Anti-V2 group compared to the other two groups, (Fig. 3D). Overall, the titers of plasma Abs binding to V1V2 scaffold proteins and cV2 peptides were comparable between controllers and non-controllers (Fig. 3E, 3F) except for the Anti-Env group titers against $cV2_{230}$ peptide (p=0.016, Fig. 3F).

One of the cV2 peptides we tested matches the $V2_{BaL}$ sequence that is also present in the $SHIV_{BaL.P4}$ challenge stock. When compared across groups as AUC, $V2_{BaL}$ Ab titers were highest in the Anti-V2 group compared to the Anti-Env (p=0.0353) or Anti-V2 Mucosal (p=0.0005) groups (Supplementary Fig. 2A), but no difference was seen between controllers and non-controllers in either group (Supplementary Fig. 2B). To evaluate whether the Ab titers we measured against the cV2 BaL peptide could have been induced after challenge and during infection, we analyzed early and late PVL timepoints in both Anti-V2 groups. However, we found no correlations between PVL and titers of plasma Abs against the $cV2_{BaL}$ peptide in the Anti-V2 and Anti-V2 Mucosal groups (Supplementary Fig. 2C, 2D). We conclude from the lack of an inverse relationship between anti-V2 Ab titers and PVL and from a lack of difference in V2 Abs titers between controllers and non-controllers that plasma Abs binding to V1V2 proteins and V2 peptides likely did not contribute to control of viremia during $SHIV_{BaL.P4}$ infection.

Plasma antibodies against cyclic $V1_{92TH023}$ peptide

The V1 region encoded by $gp160_{92TH023}$ DNA was present in the Anti-Env vaccine, and $V1V2_{92TH023}$ DNA was present in both the Anti-V2 and Anti-V2 Mucosal vaccines. In order to determine if anti-V1 Abs were induced, we tested titrated plasma samples against a biotinylated cyclic homologous $V1_{92TH023}$ peptide, given that the V1 region is exceptionally hypervariable (Fig. 4). The binding activities varied greatly among the groups with virtually no detectable anti-V1 Abs in the Anti-Env group (Fig. 4A). Thus, no control of $SHIV_{BaL.P4}$ can be attributed to anti-V1 Abs in the Anti-Env group. When analyzed as the area under the curve (AUC), the difference in titers of anti-$V1_{92TH023}$ binding Abs in the Anti-V2 group compared to either the Anti-Env or Anti-V2 Mucosal groups was highly significant (p<0.0001, Fig. 4D). However, we found no differences between controllers and non-controllers in either group, suggesting that anti-$V1_{92TH023}$ Abs were not responsible for preventing $SHIV_{BaL.P4}$ infection or viral control in any group (Fig. 4E).

Anti-V2 antibodies in mucosal secretions

Buccal and vaginal secretions were collected and samples from all three groups at TOC tested against experiment-relevant antigens. We used buccal and vaginal secretions to avoid interference with multiple IR challenges. The Anti-Env group samples were tested by

ELISA for IgG binding Abs against $gp120_{BaL}$ and $gp120_{MN}$, and samples from the Anti-V2 and Anti-V2 Mucosal groups were tested against $gp120_{BaL}$ and $V1V2_{1086}$-tags (Fig. 5). Due to the limitations of sample volume, IgA Abs were not tested. IgG Ab binding activity against $gp120_{BaL}$ and $gp120_{MN}$ was much stronger in titrated buccal and vaginal fluids of Anti-Env vaccinated macaques than the Anti-V2 groups, especially in vaginal secretions (compare Fig. 5A–B, 5G–H to 5C–F). Commensurate with V1V2 scaffold data in plasma samples, Abs were present in secretion fluids from the Anti-V2 group that strongly reacted with $V1V2_{1086}$-tags (Fig. 5I–J). Noticeably, buccal and vaginal IgG Abs in secretions were detectable from only two animals in the Anti-V2 Mucosal group (Fig. 5K–L). Across groups and irrespective of the antigen tested, IgG Abs from either buccal or vaginal secretions were comparable between controllers and non-controllers (Fig. 5M–5R), indicating that Abs against gp120 and V2 in mucosal secretions were not controlling the $SHIV_{BaL.P4}$ infection.

Virus neutralization by plasma antibodies

We measured neutralizing plasma Abs (NAbs) longitudinally throughout the vaccine and challenge phases in each group. Only the Anti-Env vaccine induced NAbs against the challenge virus, $SHIV_{BaL.P4}$ (Fig. 6A). NAbs were not detected in either the Anti-V2 or Anti-V2 Mucosal groups against any viruses tested (data not shown). In the sham vaccinated control animals challenged concurrently with the Anti-Env group, peak PVL occurred at or near week 24, two weeks post TOC (Fig 2A). In contrast, at this time point, all but one animal (32238) in the Anti-Env group developed 50% neutralizing (ID_{50}) >1,000 against the challenge strain, ranging from 1,077 to 5,837, that inversely correlated with PVL (p=0.0357) (Fig. 6B).

Neutralization by plasma Abs at week 22 (TOC) was tested against seven other pseudotyped viruses, including the clade C, tier 1 SHIV-1157ipEL. Anti-Env neutralizing titers against SHIV-1157ipEL were similar to those against the challenge virus (Fig. 6C). In addition, the Anti-Env plasma Abs neutralized the HIV-1 Tier 1-pseudotyped viruses SF162, (clade B), Q461d1, Q23env17 (clade A) and DJ263.8 (02_AG); while ZM109 (clade C) was resistant (Fig. 6C). The only Tier 2 virus neutralized was JRCSF (clade B). During the vaccine phase of the experiment, neutralizing titers of controllers and non-controllers were comparable against all viruses tested (Supplementary Fig. 3A). A clear and significant difference is seen between these two sub-groups after challenges begin and continuing through necropsy at week 35 with lower neutralization in the controllers (p=0.0159, Fig. 6D). This difference reflects the extremely low or absent persistent antigen in the controllers, and thus no additional increases in neutralization titers developed. Although only a weak inverse correlation was found between $SHIV_{BaL.P4}$ NAbs and PVL, it suggests that the vaccine-induced plasma NAbs may account for the lack of viremia in Anti-Env controllers.

The Anti-V2 vaccine consisted of both the V1 and V2 regions of HIV Env (92TH023, A244) that could potentially induce V1 Abs and neutralize viruses homologous to the immunogens. To test whether any Anti-V1 vaccine-specific NAbs were induced, we assayed the plasma samples against HIV-1 Tier 1, 92TH023.6 and Tier 2, CM244.c01 (Table III). Plasma samples from all animals in the Anti-Env group neutralized the Tier 1 virus 92TH023.6 with titers ranging from 592 to 4,277. In contrast, plasma Abs from the Anti-V2 study were very

weak against 92TH023.6 and considered non-neutralizing based on the criterion requiring a greater than three-fold increase in activity compared with the SVA-MLV negative control pseudovirus. Anti-Env group plasma weakly neutralized the Tier 2 virus CM244.c01 with titers >50 in only one of the nine animals (Table III) and showed no correlation with $SHIV_{BaL.P4}$ NAbs (Supplementary Fig. 3C). No CM244.c01 neutralization was detected in any of the animals in the Anti-V2 study (Table III). Binding Abs against the $cV1_{92TH023}$ peptide, $V1V2_{A244}$ or $cV2_{A244}$ peptide did not correlate with NAbs against $SHIV_{BaL.P4}$ (Supplementary Fig. 3B, 3D, 3E, respectively). We conclude that, unlike the Anti-V2 and Anti-V2 Mucosal groups, NAbs against $SHIV_{BaL.P4}$ induced by the Anti-Env vaccine likely influenced the control of infection.

ADCC and ADCP activities of plasma Abs

We tested macaque plasma samples from the Anti-Env and Anti-V2 groups at week 22 against $SHIV_{SF162P3}$-infected cells in an ADCC assay using an NK cell line expressing rhesus CD16 as effector cells. Cytotoxic activity is represented by a reduction in relative light units (RLUs) with a plasma dilution resulting in 50% cell death considered the threshold for activity. Plasma Ab ADCC activity varied in each group with only two animals in the Anti-Env group (33617, 33620) and four animals (33788, 33863, 34151, 34209) in the Anti-V2 group reaching the 50% threshold for ADCC activity at the lowest dilutions (Fig. 7A, 7B). When calculated as AUC, there was no difference between non-controllers and controllers in either group (Fig. 7E), and ADCC activity did not correlate with PVL at week 24 (Supplementary Fig. 4A, 4B) or with NAbs against the challenge virus (Supplementary Fig. 4C).

We also examined ADCP of plasma samples from the Anti-Env and Anti-V2 groups at four dilutions (1:25–1:200), using beads coated with $gp120_{BaL}$ (Fig 7C, 7D). In both studies, Anti-Env and Anti-V2, the phagocytic activity measured by AUC was significantly higher at TOC (week 22) compared to pre-vaccination, day 0 ($p=0.0028$, $p=0.0083$, respectively), indicating that the immunization strategy induced Abs capable of mediating phagocytosis (Supplementary Fig. 4D, 4E). AUC of ADCP activity was comparable between controllers and non-controllers in both studies (Fig. 7F), suggesting that Abs mediating phagocytosis did not correlate with $SHIV_{BaL.P4}$ acquisition. Taken together, the data indicate that neither ADCC nor ADCP was associated with SHIV acquisition or control.

ADCVI activity of plasma antibodies against $SHIV_{BaL.P4}$-infected target cells

Plasma samples from each group were tested longitudinally throughout the immunizations (weeks 0, 14, 22) at a dilution of 1:100 for ADCVI. We measured higher ADCVI activity in the Anti-Env group than the Anti-V2 or the Anti-V2 Mucosal groups, with the lowest activity seen in the Anti-V2 group (Fig 8A–C). Measured as AUC, the ADCVI activity at week 22 in both the Anti-Env group and the Anti-V2 Mucosal group was significantly higher compared to the Anti-V2 group ($p=0.0188$, $p=0.0012$, respectively) (Fig. 8D). When analyzed to compare controllers and non-controllers, ADCVI activity was comparable in all three groups, suggesting that this function was not involved in the control of $SHIV_{BaL.P4}$ infection (Fig. 8E).

Antibody capture of infectious $SHIV_{BaL.P4}$

We tested plasma samples collected at weeks 0, 14, and 22 in a virus capture assay using the $SHIV_{BaL.P4}$ challenge virus (Fig. 9). Capture Abs increased between weeks 14 and 22 (2 weeks after immunizations 3 and 4) in all three groups, and the groups' comparison reveals that Abs from the Anti-Env group at week 14, 22 captured significantly more virus than the Anti-V2 or Anti-V2 Mucosal groups (p=0.006) (Fig. 9A). Capture Abs in the Anti-V2 and Anti-V2 Mucosal groups were comparable at weeks 14 and 22. At TOC, week 22, the Anti-Env group had significantly more $SHIV_{BaL.P4}$ capture Abs than the Anti-V2 group (p=0.0028) (Fig. 9B).

We also compared SHIV $_{BaL.P4}$ capture Abs to $cV2_{BaL}$ peptide-binding Abs in the Anti-Env and Anti-V2 groups. Our goal was to determine if we could detect a qualitative difference in plasma Abs induced by the Anti-Env vaccine compared to the Anti-V1V2 vaccine. At the TOC, binding Ab titers to $cV2_{BaL}$ peptide were comparable between the Anti-Env and Anti-V2 groups (Fig. 9C). Different assays determined capture and binding Abs. Therefore, to compare the groups more functionally, we calculated a ratio of $SHIV_{BaL.P4}$ capture Abs to titers of $cV2_{BaL}$ peptide-binding Abs. Titers of $cV2_{BaL}$ binding Abs between the groups were similar with a ratio of 0.4. In contrast, the ratio of capture Abs between the groups was 31, representing a much greater proportion of Anti-Env Abs recognizing Env on infectious virions (Fig. 9B, 9C). These results indicate that anti-V2 Abs in both groups bind to the linear epitope of the $cV2_{BaL}$ peptide equally well, but the groups differ significantly in the ability to capture $SHIV_{BaL.P4}$ virions.

To evaluate whether the capture Abs in the Anti-Env group influenced SHIV pathogenesis or virus control, we compared vaccine-induced $SHIV_{BaL.P4}$ capture Abs at TOC (week 22) in each group and compared controllers to non-controllers. Capture Abs in the Anti-Env group were greater in controllers (p=0.0317) (Fig. 9D) and correlated inversely with PVL at week 26 (p=0.0013) (Fig. 9E). In contrast, capture Abs in the Anti-V2 and Anti-V2 mucosal groups were comparable between controllers and non-controllers and no correlation with PVL was observed (data not shown). We found a correlation between Anti-Env capture Abs elicited by the third immunization (samples from week 14) and ADCVI activity at week 22 (p=0.0124, Fig 9F).

In summary, polyclonal virus capturing and NAbs against the challenge virus, $SHIV_{BaL.P4}$, suggest two immune correlates for the Anti-Env experiment that were not detected in either the Anti-V2 or Anti-V2 Mucosal groups, indicating that V2 Abs acting alone or mediating cellular functions were not associated with control of $SHIV_{BaL.P4}$ viremia.

Discussion

This study was designed to test whether V1V2 vaccine-induced anti-V2 Abs could protect against heterologous Tier 1 $SHIV_{BaL.P4}$ challenge in rhesus macaques. The results revealed that a vaccine eliciting neutralizing and virus-capturing Abs was more likely to provide tight virus control than titers of V2 Abs without these functions. No significant difference was observed between titers of V2 Abs to various V1V2 scaffolds and cyclic V2 peptides of controllers and non-controllers in all three groups. Buccal and vaginal secretions were

comparable between controllers and non-controllers, and plasma Abs from the Anti-V2 studies did not neutralize the $SHIV_{BaL.P4}$ virus. $SHIV_{BaL.P4}$ virions were weakly captured by plasma V2 Abs from the Anti-V2 and Anti-V2 Mucosal groups, and significantly less so than by Abs from the Anti-Env group. ADCC and ADCVI activities against target cells infected with $SHIV_{SF162P3}$ and ADCP against $gp120_{BaL}$-coated beads were very modest, with no difference between controllers and non-controllers. A caveat to our ADCC assay is that while the macaque Abs are tested for cytotoxicity against a human NK cell line transduced to express rhesus CD16, it may not fully represent the activity of macaque effector cells *in vivo*. Nonetheless, we conclude that in macaques, the vaccine-induced V2 Abs in this study could not sufficiently inhibit virus either by neutralization or by Fc-mediated activity. Given that the clinical trial and experiments in rhesus macaques testing the immune response to a mosaic HIV-1 vaccine were comparable (51), our results in macaques suggest that a high level of binding V2 Abs, one of the correlates in the RV144 trial, may be a surrogate marker for another immune response mediating protection from infection as has been proposed in other macaque studies (51–54).

The level of plasma V2 Abs is associated with an HIV-infected individuals' general ability to mount an Ab response to Env proteins. The level of V2 Abs in a cohort of chronically HIV-infected subjects strongly correlated with the levels of Abs against gp120 ($p<0.0001$) and gp41, and the titer of anti-gp120 Abs was significantly lower in patients with deficient anti-V2 Abs than in donors with high titer and cross-reactive V2 Abs (55). Thus, those participants in the RV144 vaccine trial with high V2 Ab levels were likely good immune responders, and other activities could have contributed to the observed protection, e.g., mucosal Abs or secondary correlates such as neutralizing Abs and ADCC.

Several studies have been performed in rhesus macaques to test the efficacy of different vaccine regimens. These studies also analyzed the relationship between the level or titer of V2 Abs and the outcome of viral infection. There have been two classes of protection experiments, the first using HIV-1 Env antigens for vaccination, followed by SHIV challenge, and the second using SIV Env, followed by SIV infection. The two classes have yielded different results regarding the function of V2 Abs. Studies using the HIV Env immunogens and SHIV challenge protocol did not report a correlation between V2 Abs and reduced virus acquisition (17, 18, 51). In another study, using two similar protocols, the association between V2 Abs and outcome was only detected when using vaccines with the replicating simian adenovirus (SAd7) vector, but not with the non-replicating human Ad4 (44).

The second class of protection experiments, using the SIV Env immunogens and SIV challenge protocol, yielded mixed results regarding the correlation between V2 Abs and the risk of virus infection. Correlation between V2 Abs and protection was reported in five studies, including two in which the correlation depended on the adjuvant used or whether the V2 Abs were measured in mucosal secretions or serum (52, 53, 56–58). Four other studies reported no impact of the V2 Abs on virus acquisition (54, 59–61). Several of these studies suggested that V2 Abs could be a surrogate for another immune response (51–54).

One reason for the difference between these two classes of protection experiments might be the higher immunogenicity of the V2 region in SIV relative to HIV-1. This could be related to the pair of V2 cysteine residues at positions 183 and 191 that play a role in stabilizing the Env trimer (62). Vaccination of nonhuman primates with SIVmac239 and SIVsmE660 Env antigens induces much higher V2 Abs than immunization with HIV-1 Env with sequences of A244, TH023, MN, 1086, and ZM651 viruses (63).

Sequencing *env* genes of plasma viruses from nine non-controllers derived from the Anti-Env and Anti-V2 group animals revealed a number of mutations that resulted from the pressure of *de novo* Abs developed during $SHIV_{BaL.P4}$ infection and not from vaccine-elicited Abs (Table II). Our conclusion is based on (i) the presence of 11 point mutations outside of the V2 region in the Anti-V2 group that received only V1V2 immunogens, (ii) mutations from the control animal that was challenged, but not immunized, and (iii) mutations in the V1 region that could be induced only by homologous V1 sequence-specific Abs, while the vaccine was heterologous to the virus challenge.

Ten of 21 (48%) mutations in plasma viruses were located in the C2 domain, and three others in the C3 and C4 domains, most likely elicited by CD4bs and CD4-induced Abs. A range of 1–3 mutations were detected in four regions: C1, V1, V2 and V3. As the CD4bs was mainly under immune pressure, it is interesting to note that it was also under immune pressure determined by sieve analysis of breakthrough HIV-1 in the HVTN 505 clinical trial (64).

There were two mutations in the V2 region. In one virus isolated from a macaque in the Anti-Env study, two residues were deleted from the hypervariable part of the V2 region, NN189/190. This could only have been induced by the homologous anti-$SHIV_{BaL.P4}$ Abs, but not by Abs induced by immunogens with heterologous sequences. A second mutation was located in the conserved part of the V2 region, K168E. This mutation was most likely induced by immune pressure from the challenge virus in the Anti-V2 study and eventually initiated by the vaccine-induced V2 Abs because all immunogens contain K at Env position 168 (Table II).

The minimal selective pressure of V2 Abs can be explained by their weak ability to bind and capture $SHIV_{BaL.P4}$ virions. We found that V2 Abs from both the Anti-Env group and the Anti-V2 group bind to the $cV2_{BaL}$ peptide equally well (Fig. 9C), but the Anti-V2 Abs captured significantly fewer $SHIV_{BaL.P4}$ virions compared to Anti-Env Abs (Fig. 9B). The poor binding of V2 Abs to intact virions is caused by glycans shielding the V2 region and its exceptional flexibility (65, 66). Thus, capturing virions by Abs is probably more biologically relevant than measuring binding to proteins and/or peptides.

These results differ from the sieve analysis of breakthrough viruses in RV144 that detected two amino acid positions at 169 and 181 in V2 that were deemed to be associated with vaccine-induced immune responses (67). First, given that plasma viruses were analyzed at the time of HIV-1 diagnosis, the Abs induced by the infecting virus – not by the vaccine – may have led to these changes in Env sequences, comparably as we discussed above for our study. Second, Tier 1 $SHIV_{BaL.P4}$ may provide more accessibility for V2 Ab binding than

the Tier 2 CRF01-AE in RV144. However, our $SHIV_{BaL.P4}$ capture assay showed that V2 Abs captured Tier 1 virions poorly, suggesting that capturing Tier 2 viruses could be even weaker, thus resulting in limited pressure on the V2 region (Fig. 9B). Finally, matching a sieve analysis of breakthrough viruses with the titer of plasma V2 Abs would be interesting because chronically HIV-infected individuals harbor a broad range of V2 Abs, including those with no V2 Abs over many years (55).

The study was focused on vaccine-induced potentially protective V2 Abs, and the results showed that control of $SHIV_{BaL.P4}$ infection was diminished without neutralization or virus capturing capabilities, and virus spread into draining lymph nodes was not different from that of controls. However, several animals in the Anti-V2 and Anti-V2 Mucosal groups controlled the $SHIV_{BaL.P4}$ challenge. Although we did not test for other immune correlates, it is possible that innate immunity could contribute to viral control during repeated low-dose SHIV challenges. Innate immunity has no antigen specificity or memory, but some stimuli can prime monocytes and macrophages and train the cells to respond to future antigen, contributing to partial protection (68, 69). This hypothesis is supported by data showing that a mucosal vaccine protected several rhesus macaques against Tier 1 $SHIV_{SF162P4}$ without inducing any gp120 Abs. In that study, immune correlates included innate myeloid cell accumulation, monocytes, and macrophages in the colorectal mucosa that produced TNF-α, IL-6, as well as MIP1α (69). In another study of rhesus macaques immunized with SIV Env immunogens and challenged with SIV, $CD14^+$ innate monocytes were associated with a reduced risk of SIV_{mac251} acquisition (59).

In summary, the V1V2 immunogens in this study induced non-neutralizing V2 Abs in rhesus macaques that provided no immune correlation within the parameters tested for the six macaques controlling infection in the presence of weak Fc-mediated activities, and poor virus capture against $SHIV_{BaL.P4}$. The HIV-1 Env immunogens resulted in neutralizing and virus-capturing Abs that correlated with virus control in the majority of animals. The data support the concept that to increase HIV vaccine efficacy, emphasis should continue to favor induction of a broad adaptive immune response, including neutralizing activity, while boosting trained innate immunity.

Supplementary Material

Refer to Web version on PubMed Central for supplementary material.

Acknowledgments

We thank Lily Liu, Leechun Weng and Flavia Camacho for their technical and administrative assistance. We also thank Dr. David Evans for the NK effector cell line, KHYG-1 rhCD16, and for the target cells, CEM-NKR-CCR5-sLTR-Luc (NKR24) used in the ADCC assay.

The study was supported by NIH grant AI112546 (MKG), P51 OD011092 (ONPRC), and by Quality Biological, Inc. and the Vaccine Research Program, Division of AIDS, NIAID, NIH under contract No. HHSN272201800007C.

Abbreviations used in this article:

ADCC	antibody-dependent cellular cytotoxicity

ADCP	antibody-dependent cellular phagocytosis
ADCVI	antibody-dependent cell-mediated virus inhibition
AUC	area under the curve
bNAbs	broadly neutralizing antibodies
CD4bs	CD4 binding site
CRF	circulating recombinant form
Env	envelope
PVL	plasma viral load
RLU	relative light units
SHIV	simian-human immunodeficiency virus

References

1. Haynes BF, Gilbert PB, McElrath MJ, Zolla-Pazner S, Tomaras GD, Alam SM, Evans DT, Montefiori DC, Karnasuta C, Sutthent R, Liao H-X, DeVico AL, Lewis GK, Williams C, Pinter A, Fong Y, Janes H, DeCamp A, Huang Y, Rao M, Billings E, Karasavvas N, Robb ML, Ngauy V, de Souza MS, Paris R, Ferrari G, Bailer RT, Soderberg KA, Andrews C, Berman PW, Frahm N, De Rosa SC, Alpert MD, Yates NL, Shen X, Koup RA, Pitisuttithum P, Kaewkungwal J, Nitayaphan S, Rerks-Ngarm S, Michael NL, and Kim JH. 2012. Immune-correlates analysis of an HIV-1 vaccine efficacy trial. N. Engl. J. Med. 366: 1275–1286. [PubMed: 22475592]
2. Cohen J 2020. Combo of two HIV vaccines fails its big test. Science 367: 611–612. [PubMed: 32029605]
3. Alam SM, Liao H-X, Tomaras GD, Bonsignori M, Tsao CY, Hwang KK, Chen H, Lloyd KE, Bowman C, Sutherland L, Jeffries TL Jr., Kozink DM, Stewart S, Anasti K, Jaeger FH, Parks R, Yates NL, Overman RG, Sinangil F, Berman PW, Pitisuttithum P, Kaewkungwal J, Nitayaphan S, Karasavva N, Rerks-Ngarm S, Kim JH, Michael NL, Zolla-Pazner S, Santra S, Letvin NL, Harrison SC, and Haynes BF. 2013. Antigenicity and immunogenicity of RV144 vaccine AIDSVAX clade E envelope immunogen is enhanced by a gp120 N-terminal deletion. J. Virol. 87: 1554–1568. [PubMed: 23175357]
4. Pauthner MG, Nkolola JP, Havenar-Daughton C, Murrell B, Reiss SM, Bastidas R, Prevost J, Nedellec R, von Bredow B, Abbink P, Cottrell CA, Kulp DW, Tokatlian T, Nogal B, Bianchi M, Li H, Lee JH, Butera ST, Evans DT, Hangartner L, Finzi A, Wilson IA, Wyatt RT, Irvine DJ, Schief WR, Ward AB, Sanders RW, Crotty S, Shaw GM, Barouch DH, and Burton DR. 2019. Vaccine-induced protection from homologous tier 2 SHIV challenge in nonhuman primates depends on serum-neutralizing antibody titers. Immunity 50: 241–252 e6. [PubMed: 30552025]
5. Tomaras GD, and Plotkin SA. 2017. Complex immune correlates of protection in HIV-1 vaccine efficacy trials. Immunol. Rev. 275: 245–261. [PubMed: 28133811]
6. Gorny MK, Moore JP, Conley AJ, Karwowska S, Sodroski J, Williams C, Burda S, Boots LJ, and Zolla-Pazner S 1994. Human anti-V2 monoclonal antibody that neutralizes primary but not laboratory isolates of human immunodeficiency virus type 1. J. Virol. 68: 8312–8320. [PubMed: 7525987]
7. Gorny MK, Pan R, Williams C, Wang X-H, Volsky B, O'Neal T, Spurrier B, Sampson JM, Li L, Seaman MS, Kong X-P, and Zolla-Pazner S. 2012. Functional and immunochemical cross-reactivity of V2-specific monoclonal antibodies from HIV-1-infected individuals. Virology 427: 198–207. [PubMed: 22402248]

8. Corti D, Langedijk JP, Hinz A, Seaman MS, Vanzetta F, Fernandez-Rodriguez BM, Silacci C, Pinna D, Jarrossay D, Balla-Jhagjhoorsingh S, Willems B, Zekveld MJ, Dreja H, O'Sullivan E, Pade C, Orkin C, Jeffs SA, Montefiori DC, Davis D, Weissenhorn W, McKnight A, Heeney JL, Sallusto F, Sattentau QJ, Weiss RA, and Lanzavecchia A. 2010. Analysis of memory B cell responses and isolation of novel monoclonal antibodies with neutralizing breadth from HIV-1-infected individuals. PLoS One 5: e8805. [PubMed: 20098712]

9. Liao H-X, Bonsignori M, Alam SM, McLellan JS, Tomaras GD, Moody MA, Kozink DM, Hwang KK, Chen X, Tsao CY, Liu P, Lu X, Parks RJ, Montefiori DC, Ferrari G, Pollara J, Rao M, Peachman KK, Santra S, Letvin NL, Karasavvas N, Yang ZY, Dai K, Pancera M, Gorman J, Wiehe K, Nicely NI, Rerks-Ngarm S, Nitayaphan S, Kaewkungwal J, Pitisuttithum P, Tartaglia J, Sinangil F, Kim JH, Michael NL, Kepler TB, Kwong PD, Mascola JR, Nabel GJ, Pinter A A, Zolla-Pazner S, and Haynes BF. 2013. Vaccine induction of antibodies against a structurally heterogeneous site of immune pressure within HIV-1 envelope protein variable regions 1 and 2. Immunity 38: 176–186. [PubMed: 23313589]

10. Li L, Wang X-H, Williams C, Volsky B, Steczko O, Seaman MS, Luthra K, Nyambi P, Nadas A, Giudicelli V, Lefranc MP, Zolla-Pazner S, and Gorny MK. 2015. A broad range of mutations in HIV-1 neutralizing human monoclonal antibodies specific for V2, V3, and the CD4 binding site. Mol. Immunol. 66: 364–374. [PubMed: 25965315]

11. Gorny MK 2020. Search for antiviral functions of potentially protective antibodies against V2 region of HIV-1. Hum. Vaccin. Immunother. 16: 2033–2041. [PubMed: 32701369]

12. Musich T, Li L, Liu L, Zolla-Pazner S, Robert-Guroff M, and Gorny MK. 2017. Monoclonal antibodies specific for the V2, V3, CD4-binding site, and gp41 of HIV-1 mediate phagocytosis in a dose-dependent manner. J. Virol. 91: e02325–16. [PubMed: 28122974]

13. Zolla-Pazner S, Powell R, Yahyaei S, Williams C, Jiang X, Li W, Lu S, Wang S, Upadhyay C, Hioe CE, Totrov M, and Kong X-P. 2016. Rationally designed vaccines targeting the V2 region of HIV-1 gp120 induce a focused, cross-clade-reactive, biologically functional antibody response. J. Virol. 90:10993–11006. [PubMed: 27630234]

14. Hessell AJ, Powell R, Jiang X, Luo C, Weiss S, Dussupt V, Itri V, Fox A, Shapiro MB, Pandey S, Cheever T, Fuller DH, Park B, Krebs SJ, Totrov M, Haigwood NL, Kong X-P, and Zolla-Pazner S. 2019. Multimeric epitope-scaffold HIV vaccines target V1V2 and differentially tune polyfunctional antibody responses. Cell Rep. 28: 877–895 e6. [PubMed: 31340151]

15. Mayr LM, Decoville T, Schmidt S, Laumond G, Klingler J, Ducloy C, Bahram S, Zolla-Pazner S, Moog C. 2017. Non-neutralizing antibodies targeting the V1V2 domain of HIV exhibit strong antibody-dependent cell-mediated cytotoxic activity. Sci. Rep. 7: 12655. [PubMed: 28978939]

16. Hessell AJ, Shapiro MB, Powell R, Malherbe DC, McBurney SP, Pandey S, Cheever T, Sutton WF, Kahl C, Park B, Zolla-Pazner S, and Haigwood NL. 2018. Reduced cell-associated DNA and improved viral control in macaques following passive transfer of a single anti-V2 monoclonal antibody and repeated Simian/Human Immunodeficiency Virus challenges. J. Virol. 92: e02198–17. [PubMed: 29514914]

17. Barouch DH, Stephenson KE, Borducchi EN, Smith K, Stanley K, McNally AG, Liu J, Abbink P, Maxfield LF, Seaman MS, Dugast AS, Alter G, Ferguson M, Li W, Earl PL, Moss B, Giorgi EE, Szinger JJ, Eller LA, Billings EA, Rao M, Tovanabutra S, Sanders-Buell E, Weijtens M, Pau MG, Schuitemaker H, Robb ML, Kim JH, Korber BT, and Michael NL. 2013. Protective efficacy of a global HIV-1 mosaic vaccine against heterologous SHIV challenges in rhesus monkeys. Cell 155: 531–539. [PubMed: 24243013]

18. Bradley T, Pollara J, Santra S, Vandergrift N, Pittala S, Bailey-Kellogg C, Shen X, Parks R, Goodman D, Eaton A, Balachandran H, Mach LV, Saunders KO, Weiner JA, Scearce R, Sutherland LL, Phogat S, Tartaglia J, Reed SG, Hu SL, Theis JF, Pinter A, Montefiori DC, Kepler TB, Peachman KK, Rao M, Michael NL, Suscovich TJ, Alter G, Ackerman ME, Moody MA, Liao H-X, Tomaras G, Ferrari G, Korber BT, and Haynes BF. 2017. Pentavalent HIV-1 vaccine protects against simian-human immunodeficiency virus challenge. Nat. Commun. 8: 15711. [PubMed: 28593989]

19. Duerr R, and Gorny MK. 2019. V2-specific antibodies in HIV-1 vaccine research and natural infection: controllers or surrogate markers. Vaccines (Basel) 7: 82.

20. Nakamura GR, Fonseca DP, O'Rourke SM, Vollrath AL, and Berman PW. 2012. Monoclonal antibodies to the V2 domain of MN-rgp120: fine mapping of epitopes and inhibition of alpha4beta7 binding. PLoS One 7: e39045. [PubMed: 22720026]

21. Lertjuthaporn S, Cicala C, Van Ryk D, Liu M, Yolitz J, Wei D, Nawaz F, Doyle A, Horowitch B, Park C, Lu S, Lou Y, Wang S, Pan R, Jiang X, Villinger F, Byrareddy SN, Santangelo PJ, Morris L, Wibmer CK, Biris K, Mason RD, Gorman J, Hiatt J, Martinelli E, Roederer M, Fujikawa D, Gorini G, Franchini G, Arakelyan A, Ansari AA, Pattanapanyasat K, Kong X-P, Fauci AS, and Arthos J. 2018. Select gp120 V2 domain specific antibodies derived from HIV and SIV infection and vaccination inhibit gp120 binding to alpha4beta7. PLoS Pathog. 14: e1007278. [PubMed: 30153309]

22. Arthos J, Cicala C, Martinelli E, Macleod K, Van Ryk D, Wei D, Xiao Z, Veenstra TD, Conrad TP, Lempicki RA, McLaughlin S, Pascuccio M, Gopaul R, McNally J, Cruz CC, Censoplano N, Chung E, Reitano KN, Kottilil S, Goode DJ, and Fauci AS. 2008. HIV-1 envelope protein binds to and signals through integrin alpha4beta7, the gut mucosal homing receptor for peripheral T cells. Nat. Immunol. 9:301–309. [PubMed: 18264102]

23. Cicala C, Martinelli E, McNally JP, Goode DJ, Gopaul R, Hiatt J, Jelicic K, Kottilil S, Macleod K, O'Shea A, Patel N, Van Ryk D, Wei D, Pascuccio M, Yi L L, McKinnon L, Izulla P, Kimani J, Kaul R, Fauci AS, and Arthos J. 2009. The integrin alpha4beta7 forms a complex with cell-surface CD4 and defines a T-cell subset that is highly susceptible to infection by HIV-1. Proc. Natl. Acad. Sci. U S A 106: 20877–20882. [PubMed: 19933330]

24. Di Mascio M, Lifson JD, Srinivasula S, Kim I, DeGrange P, Keele BF, Belli AJ, Reimann KA, Wang Y, Proschan M, Lane HC, and Fauci AS. 2019. Evaluation of an antibody to alpha4beta7 in the control of SIVmac239-nef-stop infection. Science 365: 1025–1029. [PubMed: 31488688]

25. Abbink P, Mercado NB, Nkolola JP, Peterson RL, Tuyishime H, McMahan K, Moseley ET, Borducchi EN, Chandrashekar A, Bondzie EA, Agarwal A, Belli AJ, Reimann KA, Keele BF, Geleziunas R, Lewis MG, and Barouch DH. 2019. Lack of therapeutic efficacy of an antibody to alpha4beta7 in SIVmac251-infected rhesus macaques. Science 365: 1029–1033. [PubMed: 31488689]

26. Iwamoto N, Mason RD, Song K, Gorman J, Welles HC, Arthos J, Cicala C, Min S, King HAD, Belli AJ, Reimann KA, Foulds KE, Kwong PD, Lifson JD, Keele BF, and Roederer M. 2019. Blocking alpha4beta7 integrin binding to SIV does not improve virologic control. Science 365: 1033–1036. [PubMed: 31488690]

27. Sneller MC, Clarridge KE, Seamon C, Shi V, Zorawski MD, Justement JS, Blazkova J, Huiting ED, Proschan MA, Mora JR, Shetzline M, Moir S, Lane HC, Chun TW, and Fauci AS. 2019. An open-label phase 1 clinical trial of the anti-alpha4beta7 monoclonal antibody vedolizumab in HIV-infected individuals. Sci. Transl. Med. 11: eaax3447. [PubMed: 31488581]

28. Burton DR, Hessell AJ, Keele BF, Klasse PJ, Ketas TA, Moldt B, Dunlop DC, Poignard P, Doyle LA, Cavacini L, Veazey RS, and Moore JP. 2011. Limited or no protection by weakly or nonneutralizing antibodies against vaginal SHIV challenge of macaques compared with a strongly neutralizing antibody. Proc. Natl. Acad. Sci. U S A 108: 11181–11186. [PubMed: 21690411]

29. Santra S, Tomaras GD, Warrier R, Nicely NI, Liao H-X, Pollara J, Liu P, Alam SM, Zhang R, Cocklin SL, Shen X, Duffy R, Xia SM, Schutte RJ, Pemble CW, Dennison SM, Li H, Chao A, Vidnovic K, Evans A, Klein K, Kumar A, Robinson J,Landucci G, Forthal DN, Montefiori DC, Kaewkungwal J, Nitayaphan S, Pitisuttithum P, Rerks-Ngarm S, Robb ML, Michael NL, Kim JH, Soderberg KA, Giorgi EE, Blair L, Korber BT, Moog C, Shattock RJ, Letvin NL, Schmitz JE, Moody MA, Gao F, Ferrari G, Shaw GM, and Haynes BF. 2015. Human non-neutralizing HIV-1 envelope monoclonal antibodies limit the number of founder viruses during SHIV mucosal infection in Rhesus Macaques. PLoS Pathog. 11: e1005042. [PubMed: 26237403]

30. Moog C, Dereuddre-Bosquet N, Teillaud JL, Biedma ME, Holl V, Van Ham G, Heyndrickx L, Van Dorsselaer A, Katinger D, Vcelar B, Zolla-Pazner S, Mangeot I, Kelly C, Shattock RJ, and Le Grand R. 2014. Protective effect of vaginal application of neutralizing and nonneutralizing inhibitory antibodies against vaginal SHIV challenge in macaques. Mucosal Immunol. 7: 46–56. [PubMed: 23591718]

31. Pissani F, Malherbe DC, Robins H, DeFilippis VR, Park B, Sellhorn G, Stamatatos L, Overbaugh J, and Haigwood NL. 2012. Motif-optimized subtype A HIV envelope-based DNA vaccines

rapidly elicit neutralizing antibodies when delivered sequentially. Vaccine 30: 5519–5526. [PubMed: 22749601]

32. Robins H, Krasnitz M, Barak H, and Levine AJ. 2005. A relative-entropy algorithm for genomic fingerprinting captures host-phage similarities. J. Bacteriol. 187: 8370–8374. [PubMed: 16321941]
33. Malherbe DC, Pissani F, Sather DN, Guo B, Pandey S, Sutton WF, Stuart AB, Robins H, Park B, Krebs SJ, Schuman JT, Kalams S, Hessell AJ, and Haigwood NL. 2014. Envelope variants circulating as initial neutralization breadth developed in two HIV-infected subjects stimulate multiclade neutralizing antibodies in rabbits. J. Virol. 88: 12949–12967. [PubMed: 25210191]
34. Mahalanabis M, Jayaraman P, Miura T, Pereyra F, Chester EM, Richardson B, Walker B, and Haigwood NL. 2009. Continuous viral escape and selection by autologous neutralizing antibodies in drug-naive human immunodeficiency virus controllers. J. Virol. 83: 662–672. [PubMed: 18987151]
35. Jiang X, Totrov M, Li W, Sampson JM, Williams C, Lu H, Wu X, Lu S, Wang S, Zolla-Pazner S, and Kong X-P. 2016. Rationally designed immunogens targeting HIV-1 gp120 V1V2 induce distinct conformation-specific antibody responses in rabbits. J. Virol. 90: 11007–11019. [PubMed: 27707920]
36. Cline AN, Bess JW, Piatak M Jr., and Lifson JD. 2005. Highly sensitive SIV plasma viral load assay: practical considerations, realistic performance expectations, and application to reverse engineering of vaccines for AIDS. J. Med. Primatol. 34: 303–312. [PubMed: 16128925]
37. Hansen SG, Ford JC, Lewis MS, Ventura AB, Hughes CM, Coyne-Johnson L, Whizin N, Oswald K, Shoemaker R, Swanson T, Legasse AW, Chiuchiolo MJ, Parks CL, Axthelm MK, Nelson JA, Jarvis MA, Piatak M Jr., Lifson JD, and Picker LJ. 2011. Profound early control of highly pathogenic SIV by an effector memory T-cell vaccine. Nature 473: 523–527. [PubMed: 21562493]
38. Hessell AJ, McBurney S, Pandey S, Sutton W, Liu L, Li L, Totrov M, Zolla-Pazner S, Haigwood NL, and Gorny MK. 2016. Induction of neutralizing antibodies in rhesus macaques using V3 mimotope peptides. Vaccine 34: 2713–27121. [PubMed: 27102818]
39. Gach JS, Venzon D, Vaccari M, Keele BF, Franchini G, and Forthal DN. 2016. Relationship between vaccine-induced antibody capture of infectious virus and infection outcomes following repeated low-dose rectal challenges with Simian Immunodeficiency Virus SIVmac251. J. Virol. 90: 8487–8495. [PubMed: 27440881]
40. Li M, Gao F, Mascola JR, Stamatatos L, Polonis VR, Koutsoukos M, Voss G, Goepfert P, Gilbert P, Greene KM, Bilska M, Kothe DL, Salazar-Gonzalez JF, Wei X, Decker JM, Hahn BH, and Montefiori DC. 2005. Human immunodeficiency virus type 1 env clones from acute and early subtype B infections for standardized assessments of vaccine-elicited neutralizing antibodies. J. Virol. 79: 10108–10125. [PubMed: 16051804]
41. Blay WM, Kasprzyk T, Misher L, Richardson BA, and Haigwood NL. 2007. Mutations in envelope gp120 can impact proteolytic processing of the gp160 precursor and thereby affect neutralization sensitivity of human immunodeficiency virus type 1 pseudoviruses. J. Virol. 81: 13037–13049. [PubMed: 17855534]
42. Alpert MD, Heyer LN, Williams DE, Harvey JD, Greenough T, Allhorn M, and Evans DT. 2012. A novel assay for antibody-dependent cell-mediated cytotoxicity against HIV-1- or SIV-infected cells reveals incomplete overlap with antibodies measured by neutralization and binding assays. J. Virol. 86: 12039–12052. [PubMed: 22933282]
43. Ackerman ME, Moldt B, Wyatt RT, Dugast AS, McAndrew E, Tsoukas S, Jost S, Berger CT, Sciaranghella G, Liu Q, Irvine DJ, Burton DR, and Alter G. 2011. A robust, high-throughput assay to determine the phagocytic activity of clinical antibody samples. J. Immunol. Methods 366: 8–19. [PubMed: 21192942]
44. Malherbe DC, Mendy J, Vang L, Barnette PT, Reed J, Lakhashe SK, Owuor J, Gach JS, Legasse AW, Axthelm MK, LaBranche CC, Montefiori D, Forthal DN, Park B, Wilson JM, McLinden JH, Xiang J, Stapleton JT, Sacha JB, Haynes BF, Liao H-X, Ruprecht RM, Smith J, Gurwith M, Haigwood NL, and Alexander J. 2018. Combination Adenovirus and protein vaccines prevent infection or reduce viral burden after heterologous clade C Simian-Human Immunodeficiency Virus mucosal challenge. J. Virol. 92: e01092–17. [PubMed: 29093095]
45. Courtney CR, Mayr L, Nanfack AJ, Banin AN, Tuen M, Pan R, Jiang X, Kong X-P, Kirkpatrick AR, Bruno D, Martens CA, Sykora L, Porcella SF, Redd AD, Quinn TC, Nyambi PN, and Durr R.

2017. Contrasting antibody responses to intrasubtype superinfection with CRF02_AG. PLoS One 12: e0173705. [PubMed: 28288209]

46. Salazar-Gonzalez JF, Bailes E, Pham KT, Salazar MG, Guffey MB, Keele BF, Derdeyn CA, Farmer P, Hunter E, Allen S, Manigart O, Mulenga J, Anderson JA, Swanstrom R, Haynes BF, Athreya GS, Korber BT, Sharp PM, Shaw GM, and Hahn BH. 2008. Deciphering human immunodeficiency virus type 1 transmission and early envelope diversification by single-genome amplification and sequencing. J. Virol. 82: 3952–3970. [PubMed: 18256145]
47. Tamura K, Peterson D, Peterson N, Stecher G, Nei M, and Kumar S. 2011. MEGA5: molecular evolutionary genetics analysis using maximum likelihood, evolutionary distance, and maximum parsimony methods. Mol. Biol. Evol. 28: 2731–2739. [PubMed: 21546353]
48. Muhl T, Krawczak M, Ten Haaft P, Hunsmann G, and Sauermann U. 2002. MHC class I alleles influence set-point viral load and survival time in simian immunodeficiency virus-infected rhesus monkeys. J. Immunol. 169: 3438–3446. [PubMed: 12218167]
49. Sauermann U, Siddiqui R, Suh YS, Platzer M, Leuchte N, Meyer H, Matz-Rensing K, Stoiber H, Nurnberg P, Hunsmann G, Stahl-Hennig C, and Krawczak M. 2008. Mhc class I haplotypes associated with survival time in simian immunodeficiency virus (SIV)-infected rhesus macaques. Genes Immun. 9: 69–80. [PubMed: 18094710]
50. Yant LJ, Friedrich TC, Johnson RC, May GE, Maness NJ, Enz AM, Lifson JD, O'Connor DH, Carrington M, and Watkins DI. 2006. The high-frequency major histocompatibility complex class I allele Mamu-B*17 is associated with control of simian immunodeficiency virus SIVmac239 replication. J. Virol. 80: 5074–5077. [PubMed: 16641299]
51. Barouch DH, Tomaka FL, Wegmann F, Stieh DJ, Alter G, Robb ML, Michael NL, Peter L, Nkolola JP, Borducchi EN, Chandrashekar A, Jetton D, Stephenson KE, Li W, Korber B, Tomaras GD, Montefiori DC, Gray G, Frahm N, McElrath MJ, Baden L, Johnson J, Hutter J, Swann E, Karita E, Kibuuka H, Mpendo J, Garrett N, Mngadi K, Chinyenze K, Priddy F, Lazarus E, Laher F, Nitayapan S, Pitisuttithum P, Bart S, Campbell T, Feldman R, Lucksinger G, Borremans C, Callewaert K, Roten R, Sadoff J, Scheppler L, Weijtens M, Feddes-de Boer K, van Manen D, Vreugdenhil J, Zahn R, Lavreys L, et al. 2018. Evaluation of a mosaic HIV-1 vaccine in a multicentre, randomised, double-blind, placebo-controlled, phase 1/2a clinical trial (APPROACH) and in rhesus monkeys (NHP 13–19). Lancet 392: 232–243. [PubMed: 30047376]
52. Barouch DH, Liu J, Li H, Maxfield LF, Abbink P, Lynch DM, Iampietro MJ, SanMiguel A, Seaman MS, Ferrari G, Forthal DN, Ourmanov I, Hirsch VM, Carville A, Mansfield KG, Stablein D, Pau MG, Schuitemaker H, Sadoff JC, Billings EA, Rao M, Robb ML, Kim JH, Marovich MA, Goudsmit J, and Michael NL. 2012. Vaccine protection against acquisition of neutralization-resistant SIV challenges in rhesus monkeys. Nature 482: 89–93. [PubMed: 22217938]
53. Vaccari M, Gordon SN, Fourati S, Schifanella L, Liyanage NP, Cameron M, Keele BF, Shen X, Tomaras GD, Billings E, Rao M, Chung AW, Dowell KG, Bailey-Kellogg C, Brown EP, Ackerman ME, Vargas-Inchaustegui DA, Whitney S, Doster MN, Binello N, Pegu P, Montefiori DC, Foulds K, Quinn DS, Donaldson M, Liang F, Lore K, Roederer M, Koup RA, McDermott A, Ma ZM, Miller CJ, Phan TB, Forthal DN, Blackburn M, Caccuri F, Bissa M, Ferrari G, Kalyanaraman V, Ferrari MG, Thompson D, Robert-Guroff M, Ratto-Kim S, Kim JH, Michael NL, Phogat S, Barnett SW, Tartaglia J, Venzon D, Stablein DM, et al. 2016. Adjuvant-dependent innate and adaptive immune signatures of risk of SIVmac251 acquisition. Nat. Med. 22: 762–770. [PubMed: 27239761]
54. Kwa S, Sadagopal S, Shen X, Hong JJ, Gangadhara S, Basu R, Victor B, Iyer SS, LaBranche CC, Montefiori DC, Tomaras GD, Villinger F, Moss B, Kozlowski PA, and Amara RR. 2015. CD40L-adjuvanted DNA/modified vaccinia virus Ankara simian immunodeficiency virus (SIV) vaccine enhances protection against neutralization-resistant mucosal SIV infection. J. Virol. 89: 4690–4695. [PubMed: 25653428]
55. Liu L, Li L, Nanfack A, Mayr LM, Soni S, Kohutnicki A, Agyingi L, Wang X-H, Tuen M, Shao Y, Totrov M, Zolla-Pazner S, Kong X-P, Duerr R, and Gorny MK. 2019. Anti-V2 antibody deficiency in individuals infected with HIV-1 in Cameroon. Virology 529: 57–64. [PubMed: 30665098]
56. Singh S, Ramirez-Salazar EG, Doueiri R, Valentin A, Rosati M, Hu X, Keele BF, Shen X, Tomaras GD, Ferrari G, LaBranche C, Montefiori DC, Das J, Alter G, Trinh HV, Hamlin C, Rao M, Dayton F, Bear J, Chowdhury B, Alicea C, Lifson JD, Broderick KE, Sardesai NY, Sivananthan SJ, Fox

CB, Reed SG, Venzon DJ, Hirsch VM, Pavlakis GN, and Felber BK. 2018. Control of heterologous Simian Immunodeficiency Virus SIVsmE660 infection by DNA and protein coimmunization regimens combined with different toll-like-receptor-4-based adjuvants in Macaques. J. Virol. 92: e00281–18. [PubMed: 29793957]

57. Gordon SN, Doster MN, Kines RC, Keele BF, Brocca-Cofano E, Guan Y, Pegu P, Liyanage NP, Vaccari M, Cuburu N, Buck CB, Ferrari G, Montefiori D, Piatak M Jr., Xenophontos AM, Venzon D, Robert-Guroff M, Graham BS, Lowy DR, Schiller JT, and Franchini G. 2014. Antibody to the gp120 V1/V2 loops and CD4+ and CD8+ T cell responses in protection from SIVmac251 vaginal acquisition and persistent viremia. J. Immunol. 193: 6172–6183. [PubMed: 25398324]
58. Gordon SN, Liyanage NP, Doster MN, Vaccari M, Vargas-Inchaustegui DA, Pegu P, Schifanella L, Shen X, Tomaras GD, Rao M, Billings EA, Schwartz J, Prado I, Bobb K, Zhang W, Montefiori DC, Foulds KE, Ferrari G, Robert-Guroff M, Roederer M, Phan TB, Forthal DN, Stablein DM, Phogat S, Venzon DJ, Fouts T, and Franchini G. 2016. Boosting of ALVAC-SIV vaccine-primed Macaques with the CD4-SIVgp120 fusion protein elicits antibodies to V2 associated with a decreased risk of SIVmac251 acquisition. J. Immunol. 197: 2726–2737. [PubMed: 27591322]
59. Vaccari M, Fourati S, Gordon SN, Brown DR, Bissa M, Schifanella L, Silva de Castro I, Doster MN, Galli V, Omsland M, Fujikawa D, Gorini G, Liyanage NPM, Trinh HV, McKinnon KM, Foulds KE, Keele BF, Roederer M, Koup RA, Shen X, Tomaras GD, Wong MP, Munoz KJ, Gach JS, Forthal DN, Montefiori DC, Venzon DJ, Felber BK, Rosati M, Pavlakis GN, Rao M, Sekaly RP, and Franchini G. 2018. HIV vaccine candidate activation of hypoxia and the inflammasome in CD14(+) monocytes is associated with a decreased risk of SIVmac251 acquisition. Nat. Med. 24: 847–856. [PubMed: 29785023]
60. Barouch DH, Alter G, Broge T, Linde C, Ackerman ME, Brown EP, Borducchi EN, Smith KM, Nkolola JP, Liu J, Shields J, Parenteau L, Whitney JB, Abbink P, Ng'ang'a DM, Seaman MS, Lavine CL, Perry JR, Li W, Colantonio AD, Lewis MG, Chen B, Wenschuh H, Reimer U, Piatak M, Lifson JD, Handley SA, Virgin HW, Koutsoukos M, Lorin C, Voss G, Weijtens M, Pau MG, and Schuitemaker H. 2015. Protective efficacy of adenovirus/protein vaccines against SIV challenges in rhesus monkeys. Science 349: 320–324. [PubMed: 26138104]
61. Pegu P, Vaccari M, Gordon S, Keele BF, Doster M, Guan Y, Ferrari G, Pal R, Ferrari MG, Whitney S, Hudacik L, Billings E, Rao M, Montefiori D, Tomaras G, Alam SM, Fenizia C, Lifson JD, Stablein D, Tartaglia J, Michael N, Kim J, Venzon D, and Franchini G. 2013. Antibodies with high avidity to the gp120 envelope protein in protection from simian immunodeficiency virus SIV(mac251) acquisition in an immunization regimen that mimics the RV-144 Thai trial. J. Virol. 87: 1708–1719. [PubMed: 23175374]
62. Bohl C, Bowder D, Thompson J, Abrahamyan L, Gonzalez-Ramirez S, Mao Y, Sodroski J, Wood C, and Xiang SH. 2013. A twin-cysteine motif in the V2 region of gp120 is associated with SIV envelope trimer stabilization. PLoS One 8: e69406. [PubMed: 23936006]
63. Shen X, Duffy R, Howington R, Cope A, Sadagopal S, Park H, Pal R, Kwa S, Ding S, Yang OO, Fouda GG, Le Grand R, Bolton D, Esteban M, Phogat S, Roederer M, Amara RR, Picker LJ, Seder RA, McElrath MJ, Barnett S, Permar SR, Shattock R, DeVico AL, Felber BK, Pavlakis GN, Pantaleo G, Korber BT, Montefiori DC, and Tomaras GD. 2015. Vaccine-induced linear epitope-specific antibodies to Simian Immunodeficiency Virus SIVmac239 envelope are distinct from those induced to the Human Immunodeficiency Virus Type 1 envelope in nonhuman primates. J. Virol. 89: 8643–8650. [PubMed: 26018159]
64. deCamp AC, Rolland M, Edlefsen PT, Sanders-Buell E, Hall B, Magaret CA, Fiore-Gartland AJ, Juraska M, Carpp LN, Karuna ST, Bose M, LePore S, Miller S, O'Sullivan A, Poltavee K, Bai H, Dommaraju K, Zhao H, Wong K, Chen L, Ahmed H, Goodman D, Tay MZ, Gottardo R, Koup RA, Bailer R, Mascola JR, Graham BS, Roederer M, O'Connell RJ, Michael NL, Robb ML, Adams E, D'Souza P, Kublin J, Corey L, Geraghty DE, Frahm N, Tomaras GD, McElrath MJ, Frenkel L, Styrchak S, Tovanabutra S, Sobieszczyk ME, Hammer SM, Kim JH, Mullins JI, and Gilbert PB. 2017. Sieve analysis of breakthrough HIV-1 sequences in HVTN 505 identifies vaccine pressure targeting the CD4 binding site of Env-gp120. PLoS One 12: e0185959. [PubMed: 29149197]
65. Nyambi PN, Mbah HA, Burda S, Williams C, Gorny MK, Nadas A, and Zolla-Pazner S. 2000. Conserved and exposed epitopes on intact, native, primary human immunodeficiency virus type 1 virions of group M. J. Virol. 74: 7096–7107. [PubMed: 10888650]

66. McLellan JS, Pancera M, Carrico C, Gorman J, Julien JP, Khayat R, Louder R, Pejchal R, Sastry M, Dai K, O'Dell S, Patel N, Shahzad-ul-Hussan S, Yang Y, Zhang B, Zhou T, Zhu J, Boyington JC, Chuang GY, Diwanji D, Georgiev I, Kwon YD, Lee D, Louder MK, Moquin S, Schmidt SD, Yang ZY, Bonsignori M, Crump JA, Kapiga SH, Sam NE, Haynes BF, Burton DR, Koff WC, Walker LM, Phogat S, Wyatt R, Orwenyo J, Wang LX, Arthos J, Bewley CA, Mascola JR, Nabel GJ, Schief WR, Ward AB, Wilson IA, and Kwong PD. 2011. Structure of HIV-1 gp120 V1/V2 domain with broadly neutralizing antibody PG9. Nature 480: 336–343. [PubMed: 22113616]

67. Rolland M, Edlefsen PT, Larsen BB, Tovanabutra S, Sanders-Buell E, Hertz T, deCamp AC, Carrico C, Menis S, Magaret CA, Ahmed H, Juraska M, Chen L, Konopa P, Nariya S, Stoddard JN, Wong K, Zhao H, Deng W, Maust BS, Bose M, Howell S, Bates A, Lazzaro M, O'Sullivan A, Lei E, Bradfield A, Ibitamuno G, Assawadarachai V, O'Connell RJ, deSouza MS, Nitayaphan S, Rerks-Ngarm S, Robb ML, McLellan JS, Georgiev I, Kwong PD, Carlson JM, Michael NL, Schief WR, Gilbert PB, Mullins JI, and Kim JH. 2012. Increased HIV-1 vaccine efficacy against viruses with genetic signatures in Env V2. Nature 490: 417–420. [PubMed: 22960785]

68. Netea MG, Quintin J, and van der Meer JW. 2011. Trained immunity: a memory for innate host defense. Cell Host. Microbe. 9: 355–361. [PubMed: 21575907]

69. Sui Y, Lewis GK, Wang Y, Berckmueller K, Frey B, Dzutsev A, Vargas-Inchaustegui D, Mohanram V, Musich T, Shen X, DeVico A, Fouts T, Venzon D, Kirk J, Waters RC, Talton J, Klinman D, Clements J, Tomaras GD, Franchini G, Robert-Guroff M, Trinchieri G, Gallo RC, and Berzofsky JA. 2019. Mucosal vaccine efficacy against intrarectal SHIV is independent of anti-Env antibody response. J. Clin. Invest. 129:1314–1328. [PubMed: 30776026]

Key points:

Vaccines were designed to induce only V1V2 antibodies in NHP before SHIV challenge.

Vaccine-induced V2 antibodies did not independently control SHIV infection.

Neutralizing and virus capture anti-Env antibodies correlated with SHIV virus control.

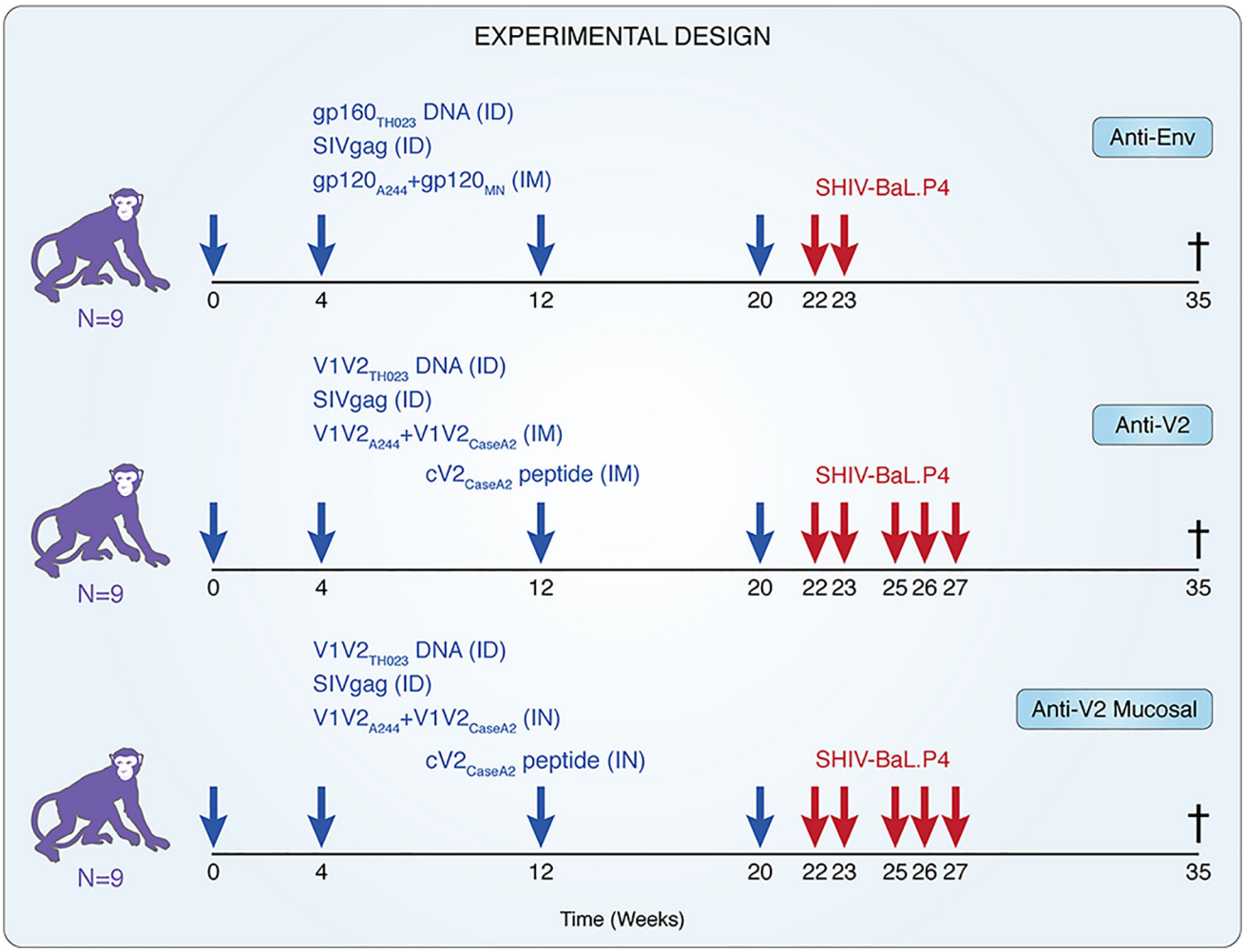

FIGURE 1. Experimental vaccine and SHIV challenge regimens.

Three groups of nine rhesus macaques were co-immunized with HIV DNA plasmid and soluble protein. At each immunization 36 μg of HIV DNA and 36μg of SIV *gag* was delivered epidermally (ID) via PMED gene gun (PowderMed, Oxford, UK) plus 100 μg of each soluble protein or peptide delivered either by intramuscular injection (IM) or intranasal atomized spray (IN) formulated with Adjuplex adjuvant as shown. DNA and protein immunogens are described for each group. Three control animals were added to each group that received a single empty plasmid sham vaccine at week 20. $SHIV_{BaL.P4}$ was administered intrarectally as indicated to all animals starting at week 22, and viral loads in plasma samples (PVL), tested in duplicate, were monitored weekly until necropsy at week 35. All controls were infected after two virus challenges in the Anti-Env group and after five challenges in the Anti-V2 and Anti-V2 Mucosal groups.

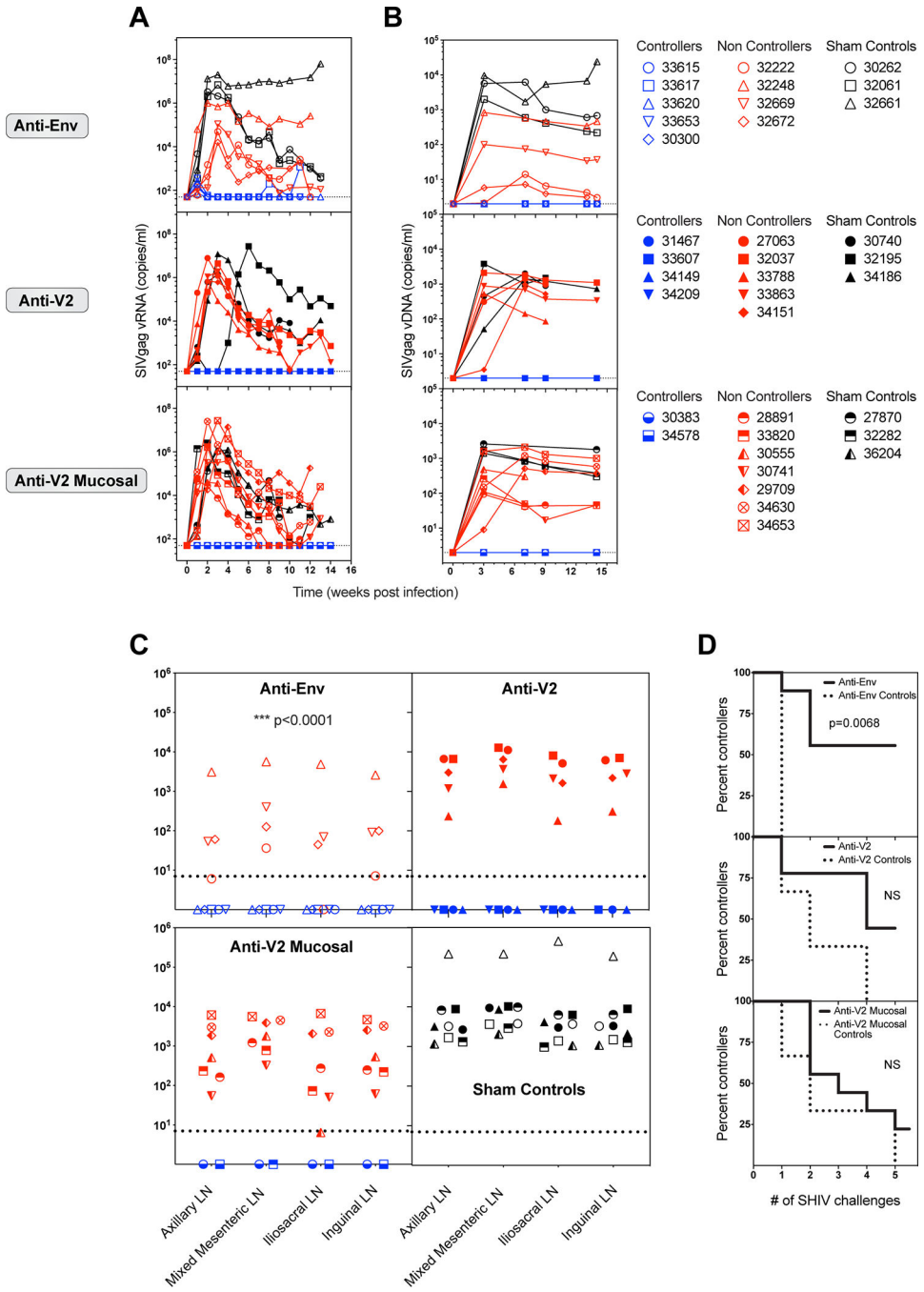

FIGURE 2. Virus loads in plasma, PBMC and tissue.

(A) SIV *gag* viral RNA in plasma samples (PVL) of all 36 macaques was followed longitudinally. PVL is graphed for each macaque individually based on the time of first detection of virus during the 16 weeks of repeated SHIV IR challenges. (B) PBMC were isolated from all 36 macaques and used to quantify cell-associated virus (CAVL), and (C) tissue associated virus was measured in duplicate in axillary, mixed mesenteric, iliosacral and inguinal lymph nodes at necropsy and reported as SIV *gag* DNA per 1×10^6 cells. The SIV vDNA was significantly increased in the Anti-V2 and Anti-V2 Mucosal groups

compared to the Anti-Env group (***p<0.0001). Unique symbols are associated with each animal and repeated in each panel. Vaccinated animals with either undetectable or low transient PVL were considered as controllers and are shown with blue symbols. Vaccinated animals with continuing PVL were considered non-controllers and have red symbols. Sham-vaccinated control animals have black symbols. (D) Adapted Kaplan-Meier curves reflect the rate of detectable PVL occurring in vaccinated macaques compared to sham-vaccinated controls in each group at each SHIV challenge. The percent of controllers, designated by no detected PVL or transient blips during repeated SHIV challenges and through the time of necropsy in each group, was 56% (Anti-Env), 44% (Anti-V2), and 22% (Anti-V2 Mucosal). Anti-Env (p=0.0068), Anti-V2 (NS), Anti-V2 Mucosal (NS) by Log-rank (Mantel-Cox) analysis.

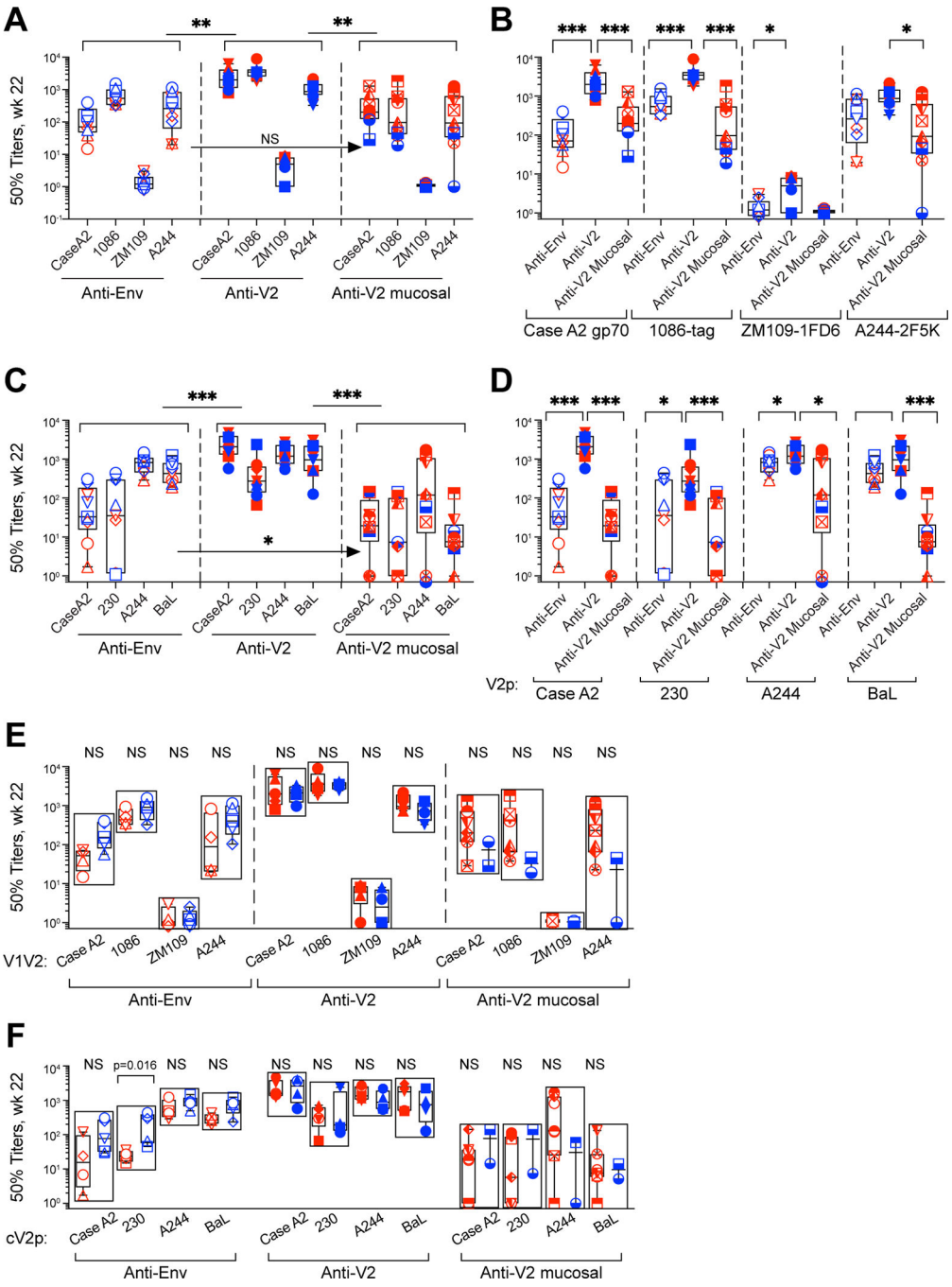

FIGURE 3. Binding of plasma antibodies against V1V2 scaffold proteins and cyclic V2 peptides and comparison of Ab titers in controllers versus non-controllers.

(A, B) The 50% maximum binding titers of plasma Abs against four V1V2 scaffold proteins, and (C, D) four cyclic V2 peptides compared by vaccine group. Titers were determined from the binding curves shown in Supplementary Fig. 1. All plasma dilutions were tested in duplicate. P values are shown *p<0.05, **p<0.01 and ***p<0.001. (E) Comparison of 50% titers of plasma V1V2 and (F) cV2p Abs in controllers (blue) versus non-controllers (red). Nonparametric Mann-Whitney test. NS – not significant. Unique animal symbols are consistent with Fig. 2.

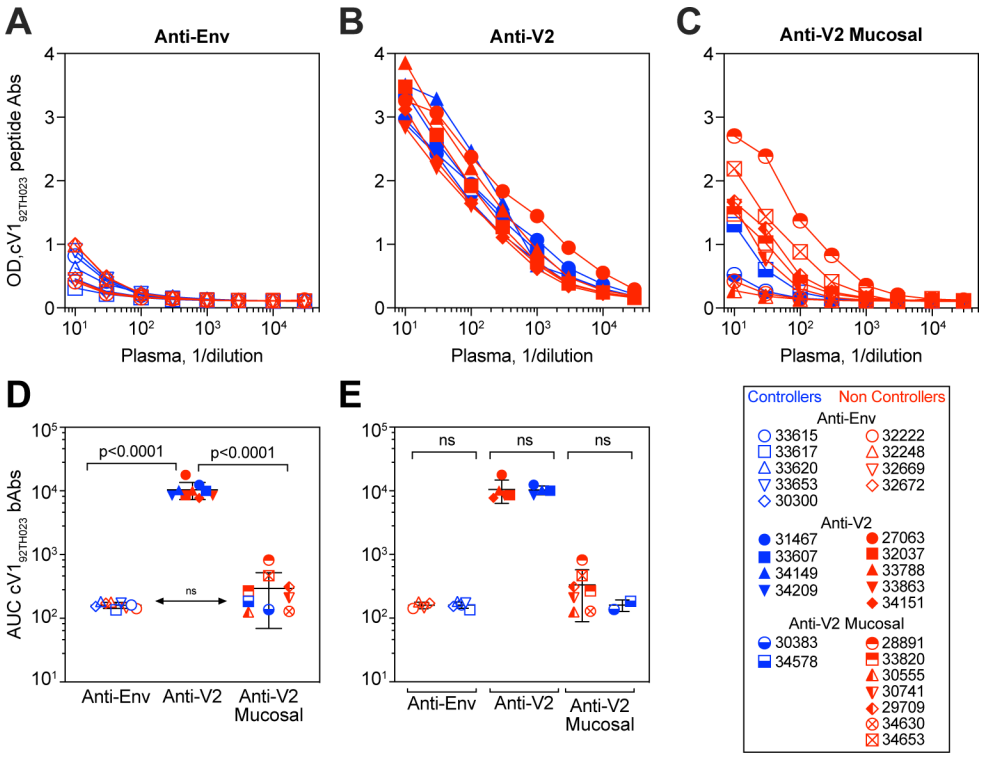

FIGURE 4. Binding of plasma antibodies to cyclic V1$_{92TH023}$ peptide.

(A) Plasma samples from week 22 (time of challenge) from Anti-Env, (B) Anti-V2 and (C) Anti-V2 Mucosal group (each group contains plasma samples from nine animals) were titrated at 1:10 to 1:30,000 dilution and tested by ELISA against biotinylated cV1$_{92TH023}$ peptide. All plasma samples were tested in duplicate. The area under the curve (AUC) of binding Ab titers are compared by group against (D) cV1$_{92TH023}$ peptide and (E) for controllers (blue) versus non-controllers (red). Data shown as median with interquartile range. Nonparametric Mann-Whitney test, NS - not significant.

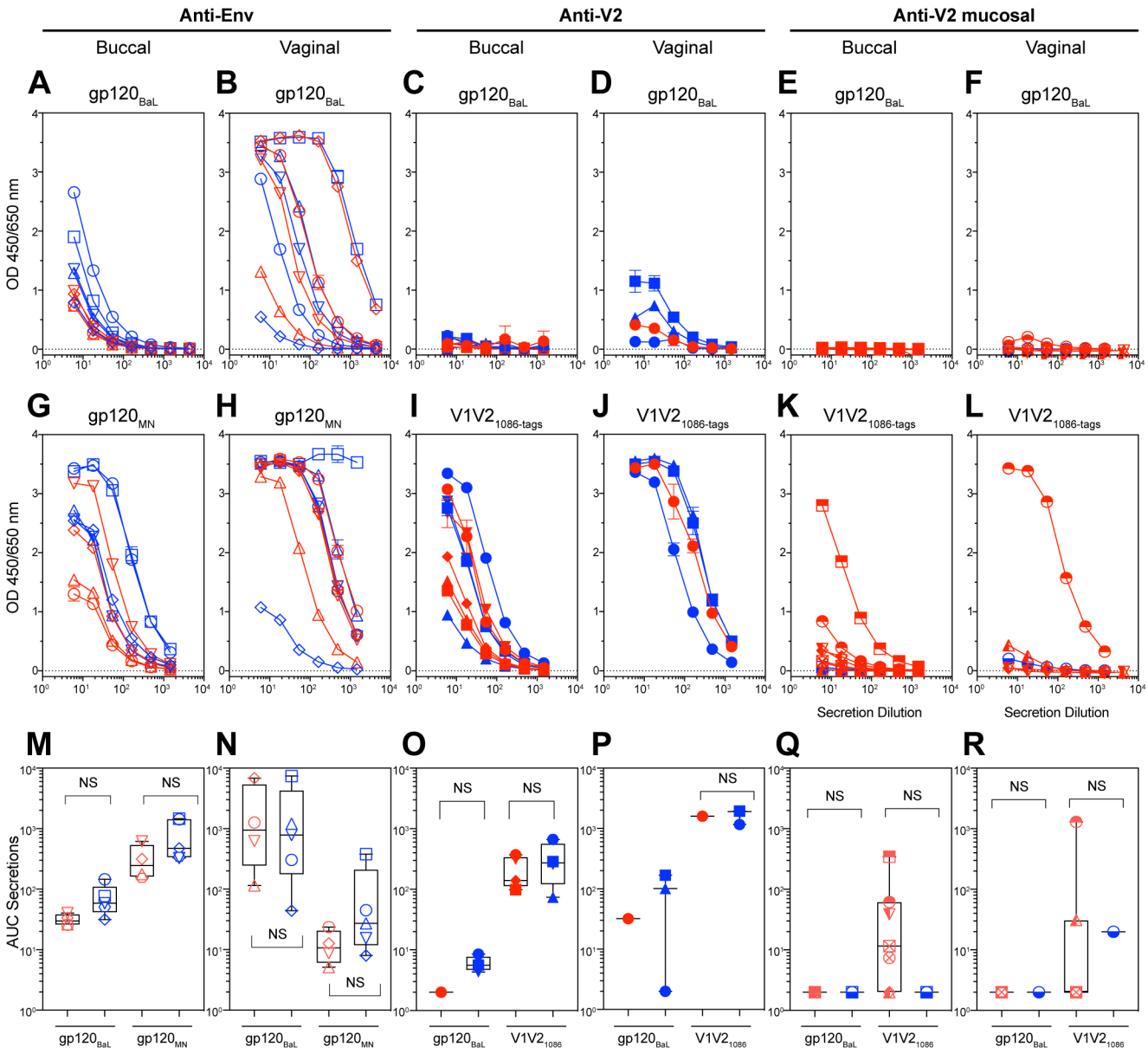

FIGURE 5. Vaccine-induced antibodies in mucosal secretions.

Buccal and vaginal mucosal secretions collected at the time of challenge (week 22) from each vaccine group were screened by ELISA against $gp120_{BaL}$ (A-F), $gp120_{MN}$ (G, H) and $V1V2_{1086}$-tags (I-L). Vaginal secretions were collected from the nine female animals in Anti-Env group, and from the five animals in Anti-V2 and Anti-V2 Mucosal groups. Mucosal secretions were tested in duplicate. (M-R) Comparison of AUCs between controllers (blue) and non-controllers (red). Nonparametric Mann-Whitney test. NS – not significant. Unique animal symbols are consistent with Fig. 2.

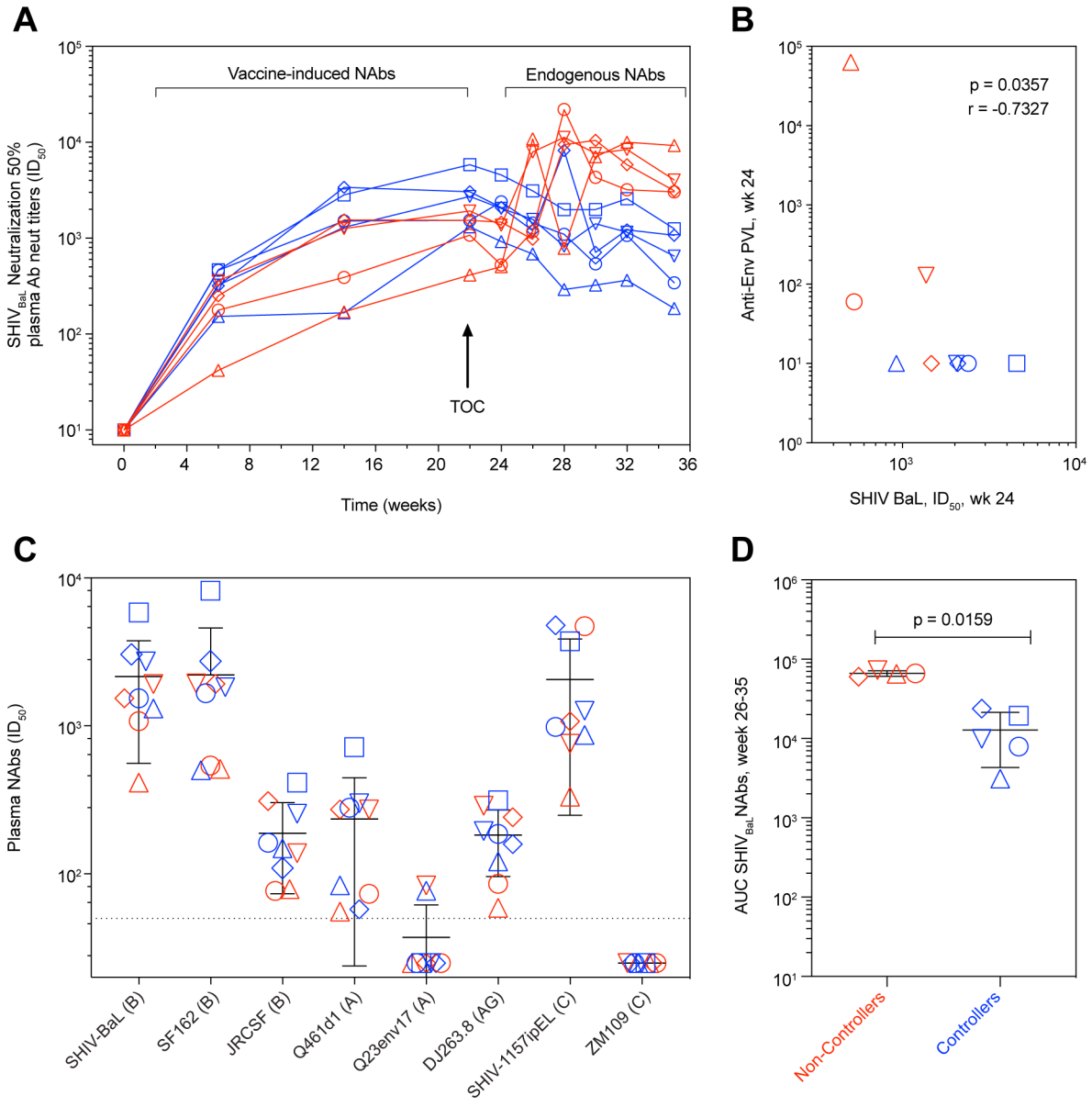

FIGURE 6. Plasma antibody neutralization of pseudotyped viruses.

The 50% inhibitory dilution (ID_{50}) was determined from plasma samples serially diluted and tested for neutralizing activities using the TZM-bl cell assay (duplicate samples, representative of two independent experiments). (A) Anti-Env group plasma longitudinal neutralization of $SHIV_{BaL.P4}$ is shown over the course of the vaccine/challenge experiment. The arrow denotes the time of challenge (TOC). (B) Inverse correlation between ID_{50} plasma neutralization and PVL at week 24. (C) Neutralization of a panel of pseudotyped viruses by Anti-Env plasma samples. Virus clades are noted in parenthesis. (D) Comparison of $SHIV_{BaL.P4}$ plasma neutralizing Abs (NAbs) in controllers (blue) vs non-controllers (red). Nonparametric Mann-Whitney test used for significance. Spearman correlation; r and P values are shown. Unique animal symbols are consistent with Fig. 2.

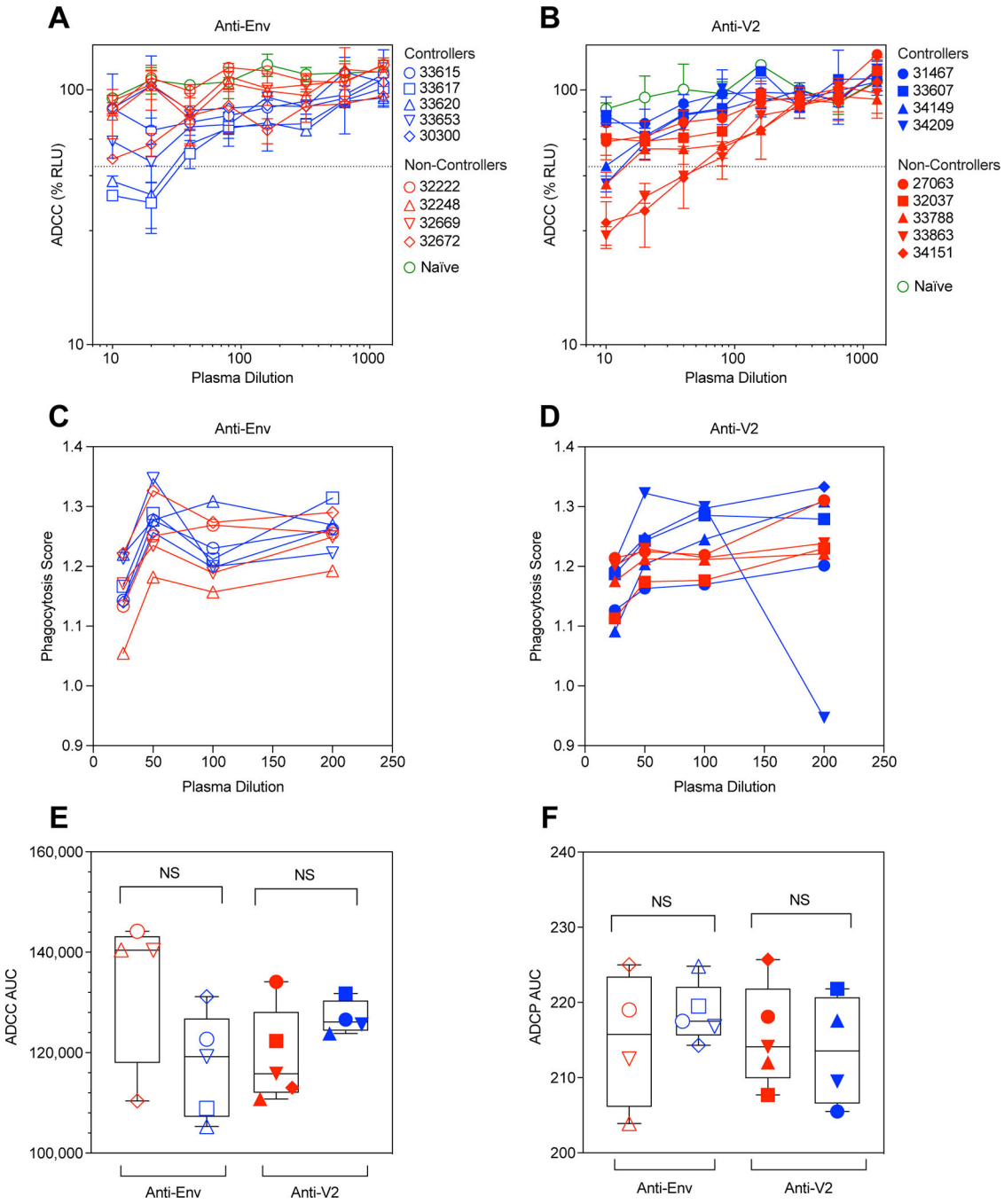

FIGURE 7. ADCC and ADCP activity of plasma antibodies.

(A) Plasma samples collected at week 22 were serially diluted and used to assess ADCC against cells infected with $SHIV_{SF162P3}$ in Anti-Env and (B) Anti-V2 experiment. A reduction in % RLUs indicates an increase in ADCC activity. Control is plasma from a naïve rhesus macaque. (C, D) Phagocytic activity of plasma Abs tested at four dilutions: 1:25 to 1:200. Phagocytosis indicates a fold increase of phagocytic scores with the $gp120_{BaL}$-coated beads over beads coated with BSA. (E) ADCC and (F) ADCP AUCs are compared between

controllers (blue) and non-controllers (red) in the Anti-Env and Anti-V2 groups. Duplicate samples, representative of two independent tests. Nonparametric Mann-Whitney test.

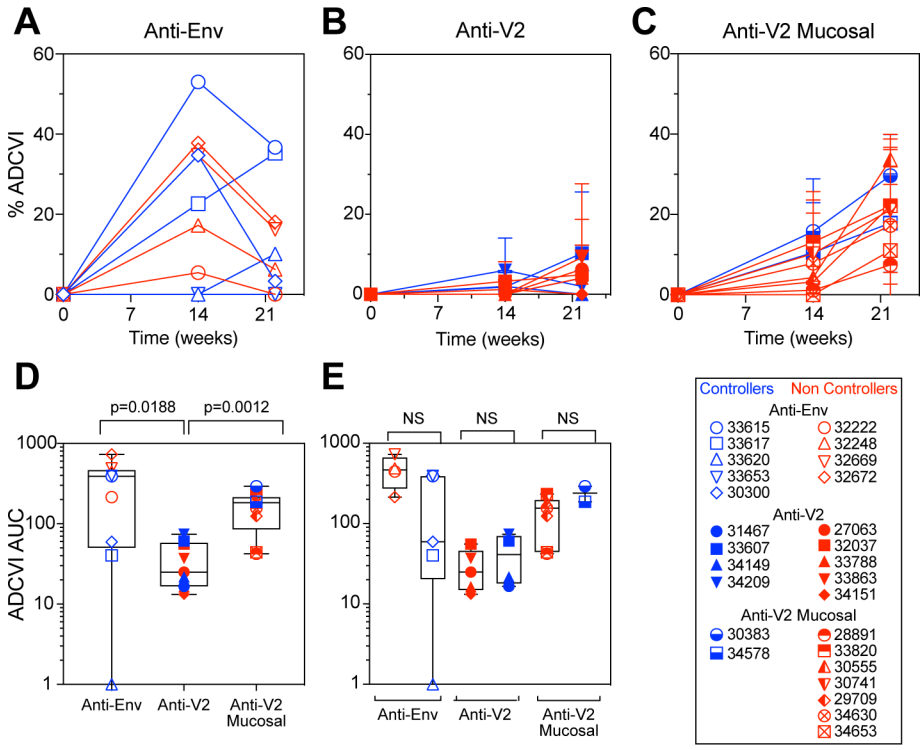

FIGURE 8. ADCVI activity in plasma samples derived from vaccinated rhesus macaques.

(A) Plasma ADCVI activity in Anti-Env, (B) Anti-V2, and (C) Anti-V2 Mucosal experiments tested at preimmunization day 0, week 14 and pre-challenge week 22. (D) Comparison of ADCVI AUC in each group. One-way ANOVA. (E) AUC compared between controllers (blue) and non-controllers (red). Duplicate samples, representative of two independent tests. Nonparametric Mann-Whitney test.

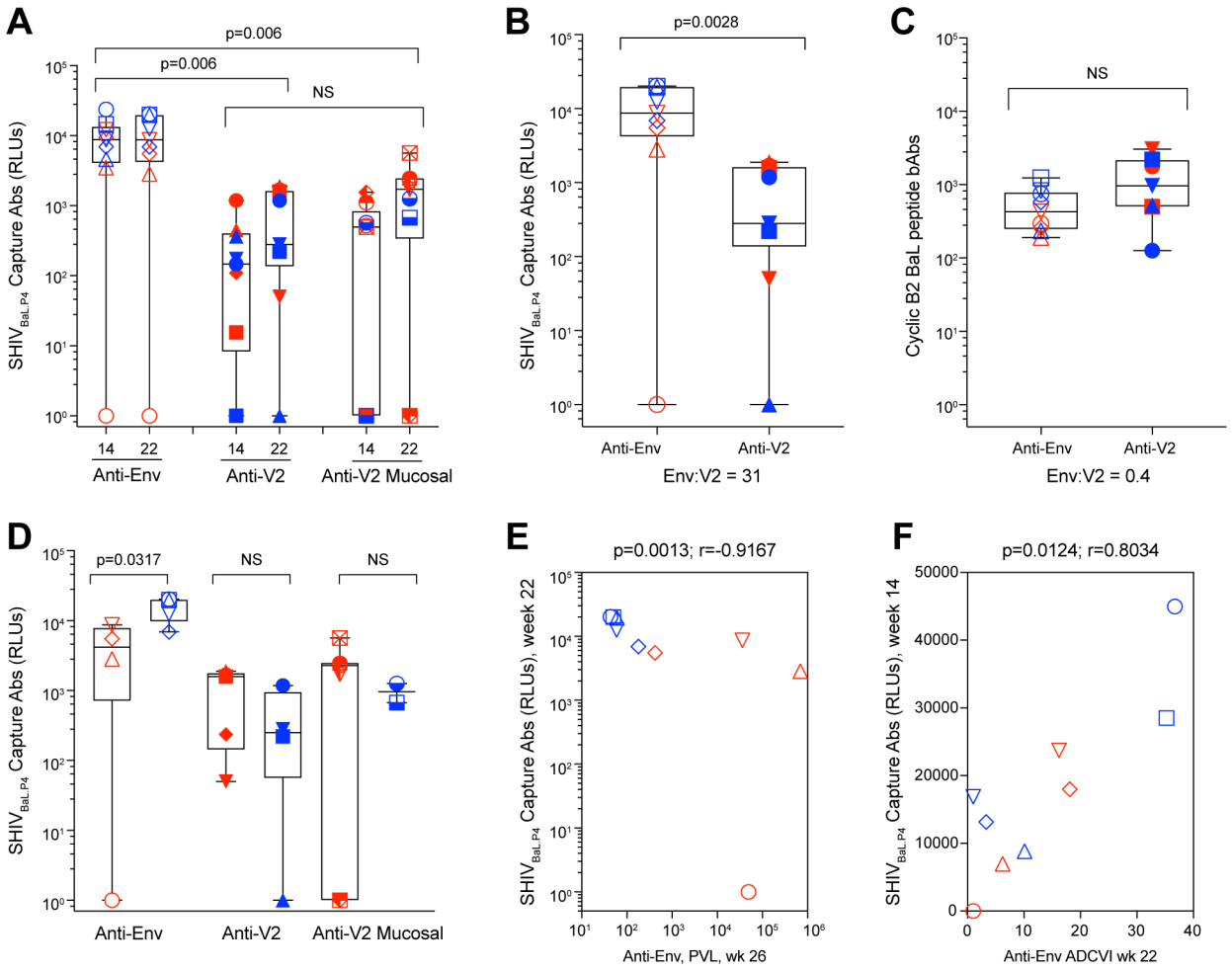

FIGURE 9. Capture of infectious $SHIV_{BaL.P4}$ by plasma antibodies from three protection experiments, Anti-Env, Anti-V2 and Anti-V2 Mucosal.

(A) $SHIV_{BaL.P4}$ was captured by rhesus macaques' immune plasma Abs at week 14 and 22 immobilized on the plates by goat anti-monkey IgG (γ) antibody. The infectivity of the captured virus was determined using TZM-bl cells. Capture is reported as relative light units (RLUs) with deduced RLU values of preimmune plasma samples at day 0. (B) RLUs of Abs capturing $SHIV_{BaL.P4}$ at week 22 from two experiments, (C) Comparison of titers of plasma Abs binding to $cV2_{BaL}$ peptide at week 22; the data are from Supplementary Fig. 1B. (B, C) The ratio of RLUs and titers for Env and V2 antibodies is 31 and 0.4, respectively. (D) Comparison of plasma Abs from controllers (blue) and non-controllers (red) at week 22 capturing $SHIV_{BaL.P4}$. (E) Level of SHIV capturing Abs, RLUs, at week 22 inversely correlated with PVL at week 26 in Anti-Env experiment, and (F) RLUs at week 14 correlated with ADCVI activity at week 22. Duplicate samples, representative of two independent tests. Nonparametric Mann-Whitney test; NS – not significant. Unique animal symbols are consistent with Fig. 2.

Table I.

MHC class I alleles in rhesus macaques[a]

ID	Mamu-A1*001:g	Mamu-A1*002:g	Mamu-B*001:g	Mamu-B*008:g	Mamu-B*017:g
		Anti-Env group			
32222	--	--	--	--	--
32248	--	--	--	--	--
32669	--	POS	POS	--	--
32672	--	POS	POS	--	--
30300	--	--	--	--	--
33615	--	--	--	--	--
33617	--	--	--	--	--
33620	--	--	--	--	--
33653	--	--	--	--	--
30262	--	--	POS	--	--
32061	--	--	POS	--	--
32661	--	--	--	--	--
		Anti-V2 group			
27063	--	--	--	--	--
32037	--	--	POS	--	--
33788	--	--	--	--	--
33863	--	--	--	--	--
34151	--	--	--	--	--
31467	POS	--	--	--	--
33607	--	--	--	--	--
34149	--	--	--	--	--
34209	--	--	--	--	--
30740	--	--	--	--	--
32195	--	--	POS	--	--
34186	--	--	--	--	--
		Anti-V2 Mucosal group			
28891	--	nt	nt	--	--
29709	--	nt	nt	--	--
30555	--	nt	nt	--	--
30741	--	nt	nt	--	--
33820	--	nt	nt	--	--
34630	--	nt	nt	--	--
34653	--	nt	nt	--	--
30383	--	nt	nt	--	--
34578	POS	nt	nt	--	--

ID	Mamu-A1*001:g	Mamu-A1*002:g	Mamu-B*001:g	Mamu-B*008:g	Mamu-B*017:g
27870	--	nt	nt	--	--
32282	--	nt	nt	--	--
36204	--	nt	nt	--	--

[a]MHC class I alleles were genotyped by sequence-specific PCR at the Macaque Genetics Core, OHSU, Beaverton, OR. Non-controllers (red); controllers (blue); sham vaccine controls (black); nt = not tested.

Table II.

Sites of immune pressure in Env revealed by mutations in plasma breakthrough viruses from non-controllers[a]

			Anti -	Env				Anti -	V2		Sham
AA (HXB2)	Site	32222	32248	32669	32672	34151	27063	32037	33788	33863	30740
22	C1										L/P,4
24	C1								I/M		
65	C1	V/E									
130	C1	N/Y									
143	V1				S/G						
147	V1			G/E							
168	V2							K/E			
189/90	V2				NN (--)						
229	C2						K/R	K/R			
254	C2		V/L	V/L	V/L	V/L	V/L				
287	C2			Q/H							
289	C2										N/S,4
290	C2									E/K	
295	C2	N/S									
312	V3		G/E								
338	C3						D/N				
375	C3							S/G			
433	C4									A/T	
839	gp41								A/T	A/T	

[a]The point mutations in the envelope protein of the breakthrough viruses were determined by analysis of the virus bulk sequence and five clones. The mutations in all six sequences from each plasma virus are shown in the table. The most common point mutation V/L occurred in five animals. The point mutations in the sham animal were present in 4 of 6 sequences.

Table III.

Neutralization activity of plasma antibodies at week 22 against pseudotyped viruses autologous to 92TH023 immunogens[a].

Animal	SVA-MLV	92TH023.6	CM244.c01
	Anti-Env	group	
32222	<20	**943**	**27**
32248	<20	**592**	**29**
32669	<20	**2429**	**75**
32672	<20	**1876**	<20
30300	22	**4277**	46
33615	<20	**539**	<20
33617	<20	**3138**	**26**
33620	<20	**1166**	**27**
33653	<20	**1656**	**46**
	Anti-V2	group	
27063	37	93	27
32037	20	28	<20
33788	24	43	21
33863	33	53	<20
34151	23	29	25
31467	29	33	28
33607	25	40	22
34149	33	24	22
34209	28	42	27

[a]Values are the serum dilution at which relative luminescence units (RLUs) were reduced by 50% compared to virus control wells (no test sample). Values in light gray boxes are background signal against the MLV-pseudotyped negative control virus. Values in bold black type are considered positive for neutralizing antibody activity based on the criterion of signal >3X the observed background against the SVA-MLV negative control pseudovirus in that sample. Non-controllers (red); controllers (blue).